High-order cell-centered DG scheme for Lagrangian hydrodynamics

F. Vilar[1], P.- H. Maire[2], R. Abgrall[3]

[1]Brown University, Division of Applied Mathematics
182 George Street, Providence, RI 02912

[2]CEA CESTA, BP 2, 33 114 Le Barp, France

[3]INRIA and University of Bordeaux, Team Bacchus,
351 Cours de la Libération, 33 405 Talence Cedex, France

September 3rd, 2013

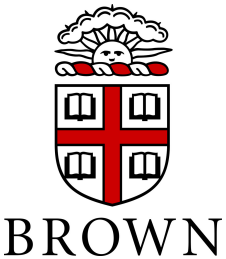

DG schemes

- Natural extension of Finite Volume method
- Piecewise polynomial approximation of the solution in the cells
- High-order scheme to achieve high accuracy

Procedure

- Local variational formulation
- Choice of the numerical fluxes (global L^2 stability, entropy inequality)
- Time discretization - TVD multistep Runge-Kutta

C.-W. SHU, *Discontinuous Galerkin methods: General approach and stability.* 2008.

- Limitation - vertex-based hierarchical slope limiters

D. KUZMIN, *A vertex-based hierarchical slope limiter for p-adaptive discontinuous Galerkin methods.* J. Comp. Appl. Math., 2009.

Circular polar grid: 10×1 cells

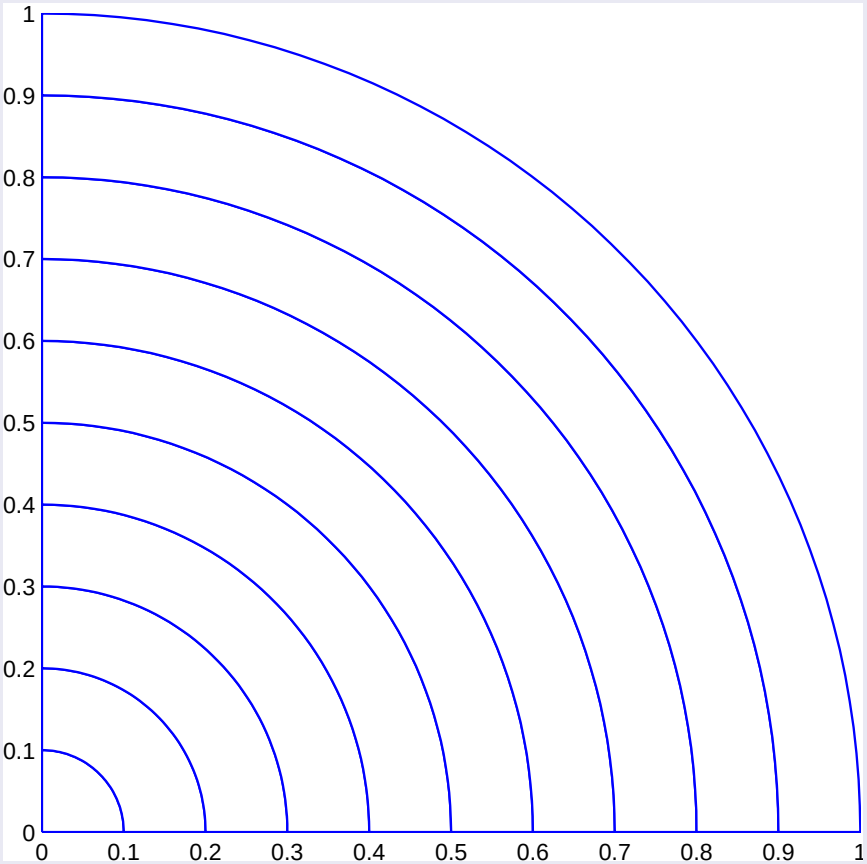

Taylor-Green exact motion

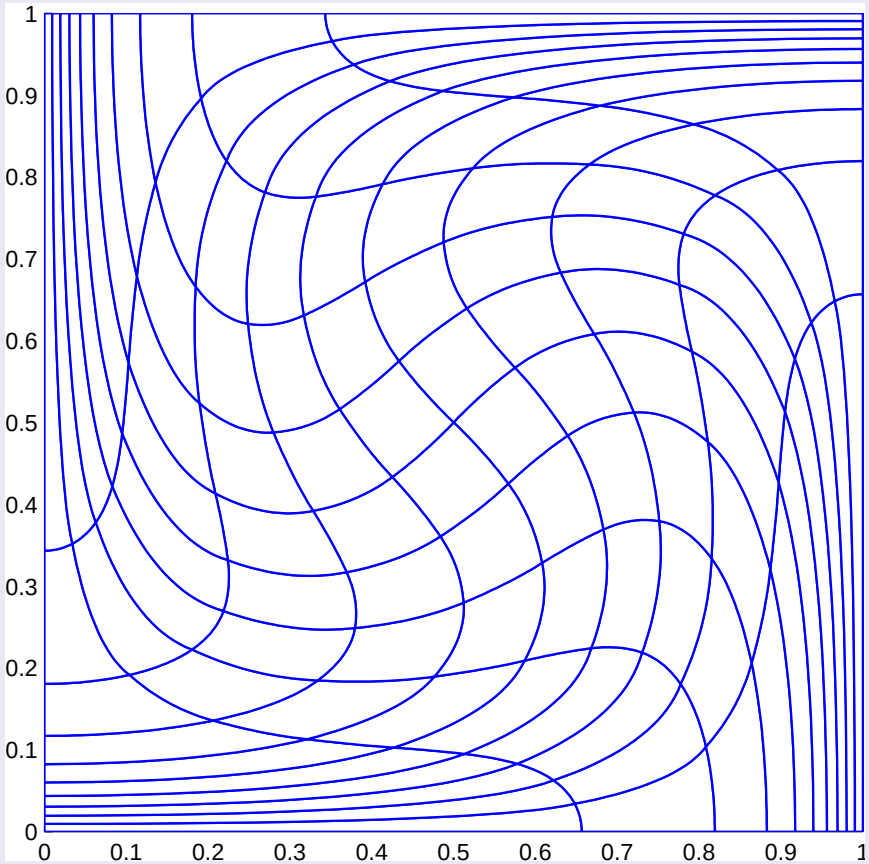

V. Dobrev, T. Ellis, T. Kolev and R. Rieben, *High Order Curvilinear Finite Elements for Lagrangian Hydrodynamics. Part I: General Framework*, 2010. Presentation available at
`https://computation.llnl.gov/casc/blast/blast.html`

Finite volume schemes on moving mesh

- J. K. Dukowicz: CAVEAT scheme
  A computer code for fluid dynamics problems with large distorsion and internal slip, 1986
- B. Després: GLACE scheme
  Lagrangian Gas Dynamics in Two Dimensions and Lagrangian systems, 2005
- P.-H. Maire: EUCCLHYD scheme
  A cell-centered Lagrangian scheme for two-dimensional compressible flow problems, 2007
- G. Kluth: Hyperelasticity
  Discretization of hyperelasticity with a cell-centered Lagrangian scheme, 2010
- S. Del Pino: Curvilinear Finite Volume method
  A curvilinear finite-volume method to solve compressible gas dynamics in semi-Lagrangian coordinates, 2010
- P. Hoch: Finite Volume method on unstructured conical meshes
  Extension of ALE methodology to unstructured conical meshes, 2011

DG scheme on initial mesh

- R. Loubère: DG scheme for Lagrangian hydrodynamics
  A Lagrangian Discontinuous Galerkin-type method on unstructured meshes to solve hydrodynamics problems, 2004

Flow transformation of the fluid

- The fluid flow is described mathematically by the continuous transformation, Φ, so-called mapping such as $\Phi : \boldsymbol{X} \longrightarrow \boldsymbol{x} = \Phi(\boldsymbol{X}, t)$

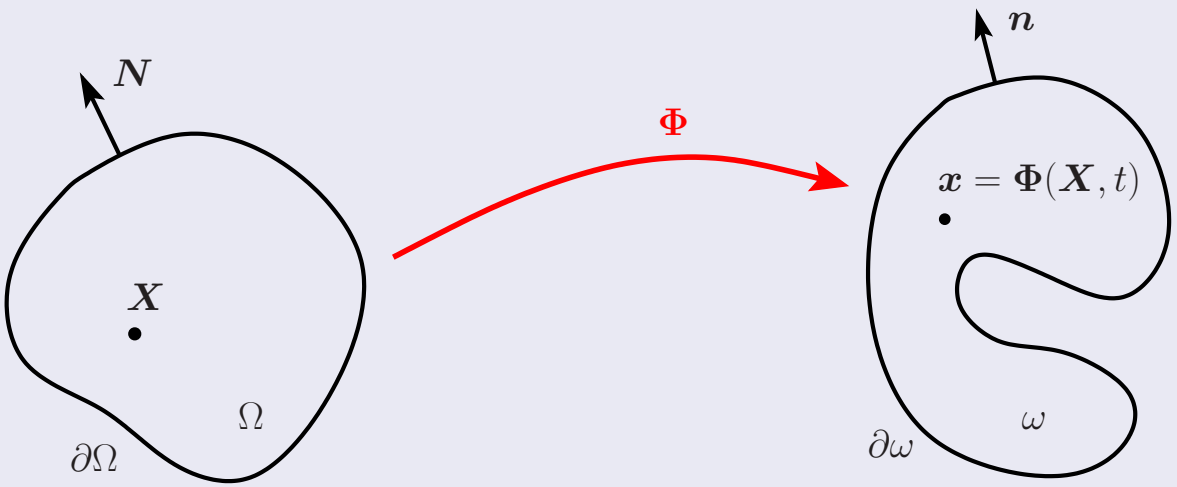

Figure: Notation for the flow map.

where $\boldsymbol{X}$ is the Lagrangian (initial) coordinate, $\boldsymbol{x}$ the Eulerian (actual) coordinate, $\boldsymbol{N}$ the Lagrangian normal and $\boldsymbol{n}$ the Eulerian normal

Deformation Jacobian matrix: deformation gradient tensor

- $\mathrm{F} = \nabla_X \Phi = \frac{\partial \boldsymbol{x}}{\partial X}$ and $J = \det \mathrm{F} > 0$

Trajectory equation

- $\dfrac{\mathrm{d}\,\boldsymbol{x}}{\mathrm{d}t} = \boldsymbol{U}(\boldsymbol{x},t), \quad \boldsymbol{x}(\boldsymbol{X},0) = \boldsymbol{X}$

Material time derivative

- $\dfrac{\mathrm{d}}{\mathrm{d}t} f(\boldsymbol{x},t) = \dfrac{\partial}{\partial t} f(\boldsymbol{x},t) + \boldsymbol{U} \,.\, \nabla_x f(\boldsymbol{x},t)$

Transformation formulas

- $\mathrm{F}\mathrm{d}\boldsymbol{X} = \mathrm{d}\boldsymbol{x}$ Change of shape of infinitesimal vectors
- $\rho^0 = \rho\, J$ Mass conservation
- $J\mathrm{d}V = \mathrm{d}v$ Measure of the volume change
- $J\mathrm{F}^{-t}\boldsymbol{N}\mathrm{d}S = \boldsymbol{n}\mathrm{d}s$ **Nanson formula**

Differential operators transformations

- $\boldsymbol{\nabla}_x P = \frac{1}{J}\nabla_X \,.\, (P\, J\mathrm{F}^{-\mathrm{t}})$ Gradient operator
- $\nabla_x \,.\, \boldsymbol{U} = \frac{1}{J}\nabla_X \,.\, (J\mathrm{F}^{-1}\boldsymbol{U})$ Divergence operator

Piola compatibility condition

- $\nabla_x \cdot G = \mathbf{0}$, where $\mathrm{G} = J\mathrm{F}^{-\mathrm{t}}$ is the cofactor matrix of F

$$\int_\Omega \nabla_x \cdot G \,\mathrm{d}V = \int_{\partial\Omega} \mathrm{G}\,\boldsymbol{N}\,\mathrm{d}S = \int_{\partial\omega} \boldsymbol{n}\,\mathrm{d}s = \mathbf{0}$$

Gas dynamics system written in its total Lagrangian form

- $\dfrac{\mathrm{d}\,\mathrm{F}}{\mathrm{d}t} - \nabla_X \boldsymbol{U} = 0$ — Deformation gradient tensor equation
- $\rho^0 \dfrac{\mathrm{d}}{\mathrm{d}t}\left(\dfrac{1}{\rho}\right) - \nabla_X \cdot (\mathrm{G}^{\mathrm{t}}\boldsymbol{U}) = 0$ — Specific volume equation
- $\rho^0 \dfrac{\mathrm{d}\,\boldsymbol{U}}{\mathrm{d}t} + \nabla_X \cdot (P\,\mathrm{G}) = \mathbf{0}$ — Momentum equation
- $\rho^0 \dfrac{\mathrm{d}\,E}{\mathrm{d}t} + \nabla_X \cdot (\mathrm{G}^{\mathrm{t}} P\boldsymbol{U}) = 0$ — Total energy equation

Thermodynamical closure

- EOS: $P = P(\rho, \varepsilon)$ where $\varepsilon = E - \frac{1}{2}\boldsymbol{U}^2$

$(s+1)^{\text{th}}$ order DG discretization

- Let $\{\Omega_c\}_c$ be a partition of the domain Ω into polygonal cells
- $\{\sigma_k^c\}_{k=0\ldots K}$ basis of $\mathbb{P}^s(\Omega_c)$, where $K+1 = \frac{(s+1)(s+2)}{2}$
- $\phi_h^c(\boldsymbol{X},t) = \sum_{k=0}^{K} \phi_k^c(t)\sigma_k^c(\boldsymbol{X})$ approximate function of $\phi(\boldsymbol{X},t)$ on Ω_c

Definitions

- Center of mass $\boldsymbol{\mathcal{X}}_c = (\mathcal{X}_c, \mathcal{Y}_c)^{\mathrm{t}} = \dfrac{1}{m_c}\displaystyle\int_{\Omega_c} \rho^0(\boldsymbol{X})\,\boldsymbol{X}\,\mathrm{d}V,$
  where m_c is the constant mass of the cell Ω_c
- The mean value $\langle\phi\rangle_c = \dfrac{1}{m_c}\displaystyle\int_{\Omega_c} \rho^0(\boldsymbol{X})\,\phi(\boldsymbol{X})\,\mathrm{d}V$
  of the function ϕ over the cell Ω_c
- The associated scalar product $(\phi\,.\,\psi)_c = \displaystyle\int_{\Omega_c} \rho^0(\boldsymbol{X})\,\phi(\boldsymbol{X})\,\psi(\boldsymbol{X})\,\mathrm{d}V$

Taylor expansion on the cell, located at the center of mass

$$\phi(\boldsymbol{X}) = \phi(\boldsymbol{\mathcal{X}}_c) + \sum_{k=1}^{s}\sum_{j=0}^{k} \frac{(X-\mathcal{X}_c)^{k-j}(Y-\mathcal{Y}_c)^{j}}{j!(k-j)!} \frac{\partial^k \phi}{\partial X^{k-j}\partial Y^{j}}(\boldsymbol{\mathcal{X}}_c) + o(\|\boldsymbol{X}-\boldsymbol{\mathcal{X}}_c\|^s)$$

$(s+1)^{\text{th}}$ order scheme polynomial Taylor basis

- The first-order polynomial component and the associated basis function

$$\phi_0^c = \langle\phi\rangle_c \quad \text{and} \quad \sigma_0^c = 1$$

- The k^{th}-order polynomial components and the associated basis functions

$$\phi^c_{\frac{k(k+1)}{2}+j} = (\Delta X_c)^{k-j}(\Delta Y_c)^{j} \frac{\partial^k \phi}{\partial X^{k-j}\partial Y^{j}}(\boldsymbol{\mathcal{X}}_c),$$

$$\sigma^c_{\frac{k(k+1)}{2}+j} = \frac{1}{j!(k-j)!}\left[\left(\frac{X-\mathcal{X}_c}{\Delta X_c}\right)^{k-j}\left(\frac{Y-\mathcal{Y}_c}{\Delta Y_c}\right)^{j} - \left\langle\left(\frac{X-\mathcal{X}_c}{\Delta X_c}\right)^{k-j}\left(\frac{Y-\mathcal{Y}_c}{\Delta Y_c}\right)^{j}\right\rangle_c\right],$$

where $0 < k \leq s$, $j = 0 \ldots k$, $\Delta X_c = \frac{X_{max}-X_{min}}{2}$ and $\Delta Y_c = \frac{Y_{max}-Y_{min}}{2}$

H. Luo, J. D. Baum and R. Löhner, *A DG method based on a Taylor basis for the compressible flows on arbitrary grids.* J. Comp. Phys., 2008.

Outcome

- First moment associated to the basis function $\sigma_0^c = 1$ is the mass averaged value

$$\phi_0^c = \langle \phi \rangle_c$$

- The successive moments can be identified as the successive derivatives of the function expressed at the center of mass of the cell

$$\phi^c_{\frac{k(k+1)}{2}+j} = (\Delta X_c)^{k-j} (\Delta Y_c)^j \frac{\partial^k \phi}{\partial X^{k-j} \partial Y^j}(\boldsymbol{x}_c)$$

- The first basis function is orthogonal to the other ones

$$(\sigma_0^c \cdot \sigma_k^c)_c = m_c \, \delta_{0k}$$

- **Same basis functions regardless the shape of the cells** (squares, triangles, generic polygonal cells)

Lagrangian gas dynamics equation type

- $\rho^0 \dfrac{\mathrm{d}\,\phi}{\mathrm{d}t} + \nabla_X \cdot (\mathrm{G}^{\mathrm{t}}\, \boldsymbol{f}) = 0,$ where $\boldsymbol{f}$ is the flux function

$\mathrm{G} = J\mathrm{F}^{-\mathrm{t}}$ is the cofactor matrix of F

Local variational formulations

- $$\int_{\Omega_c} \rho^0 \frac{\mathrm{d}\,\phi}{\mathrm{d}t} \sigma_j^c \,\mathrm{d}V = \sum_{k=0}^{K} \frac{\mathrm{d}\,\phi_k^c}{\mathrm{d}t} \int_{\Omega_c} \rho^0 \sigma_j^c \sigma_k^c \,\mathrm{d}V$$
$$= \int_{\Omega_c} \boldsymbol{f} \cdot \mathrm{G}\, \boldsymbol{\nabla}_X \sigma_j^c \,\mathrm{d}V - \int_{\partial\Omega_c} \overline{\boldsymbol{f}} \cdot \sigma_j^c \,\mathrm{G}\boldsymbol{N}\mathrm{d}S$$

Geometric Conservation Law (GCL)

- Equation on the first moment of the specific volume

$$\int_{\Omega_c} \frac{\mathrm{d}\,J}{\mathrm{d}t} \,\mathrm{d}V = \frac{\mathrm{d}\,|\omega_c|}{\mathrm{d}t} = \int_{\Omega_c} \nabla_X \cdot (\mathrm{G}^{\mathrm{t}}\, \boldsymbol{U}) \,\mathrm{d}V = \int_{\partial\Omega_c} \overline{\boldsymbol{U}} \cdot \mathrm{G}\boldsymbol{N}\mathrm{d}S$$

Mass matrix properties

- $\int_{\Omega_c} \rho^0 \sigma_j^c \sigma_k^c \, \mathrm{d}V = \left(\sigma_j^c \,.\, \sigma_k^c\right)_c$ generic coefficient of the symmetric positive definite mass matrix
- $\left(\sigma_0^c \,.\, \sigma_k^c\right)_c = m_c \, \delta_{0k}$ mass averaged equation is independent of the other polynomial basis components equations

Interior terms

- $\int_{\Omega_c} \boldsymbol{f} \,.\, \mathrm{G} \, \boldsymbol{\nabla}_X \sigma_j^c \, \mathrm{d}V$ is evaluated through the use of a two-dimensional high-order quadrature rule

Boundary terms

- $\int_{\partial\Omega_c} \overline{\boldsymbol{f}} \,.\, \sigma_j^c \, \mathrm{G} \boldsymbol{N} \mathrm{d}S$ required a specific treatment to ensure the GCL
- It remains to determine the numerical fluxes

Requirements

- **Consistency** of vector $\mathrm{G}\boldsymbol{N}\mathrm{d}S = \boldsymbol{n}\mathrm{d}s$ at the interfaces of the cells
- **Continuity** of vector $\mathrm{G}\boldsymbol{N}$ at cell interfaces on both sides of the interface
- **Preservation of uniform flows**, $\mathrm{G} = J\mathrm{F}^{-\mathrm{t}}$ the cofactor matrix

$$\int_{\Omega_c} \mathrm{G}\boldsymbol{\nabla}_X \sigma_j^c \,\mathrm{d}V = \int_{\partial\Omega_c} \sigma_j^c \,\mathrm{G}\boldsymbol{N}\mathrm{d}S \quad \Longleftrightarrow \quad \int_{\Omega_c} \sigma_j^c \,(\nabla_X \cdot \mathrm{G})\,\mathrm{d}V = \mathbf{0}$$

Generalization of the weak form of the Piola compatibility condition

Tensor F discretization

- Discretization of tensor F by means of a mapping defined on triangular cells
- Partition of the polygonal cells in the initial configuration into non-overlapping triangles

$$\Omega_c = \bigcup_{i=1}^{ntri} \mathcal{T}_i^c$$

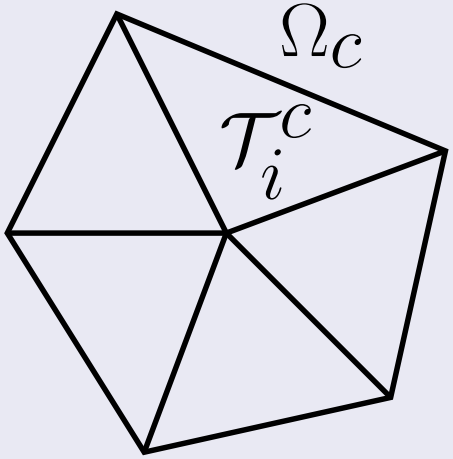

$(s+1)^{\text{th}}$ order continuous mapping function

- We develop Φ on the Finite Elements basis functions Λ_q^i in $\mathcal{T}_i$ of degree s

$$\Phi_h^i(\boldsymbol{X}, t) = \sum_{q \in \mathcal{Q}(i)} \Lambda_q^i(\boldsymbol{X})\, \Phi_q(t),$$

  where $\mathcal{Q}(i)$ is the $\mathcal{T}_i$ control points set, including the vertices $\{p^-, p, p^+\}$
- $\Phi_q(t) = \Phi(\boldsymbol{X}_q, t) = \boldsymbol{x}_q$
- $\dfrac{\mathrm{d}\,\Phi_q}{\mathrm{d}t} = \boldsymbol{U}_q \Longrightarrow \dfrac{\mathrm{d}}{\mathrm{d}t}\mathrm{F}_i(\boldsymbol{X}, t) = \sum_{q \in \mathcal{Q}(i)} \boldsymbol{U}_q(t) \otimes \boldsymbol{\nabla}_X \Lambda_q^i(\boldsymbol{X})$

G. KLUTH AND B. DESPRÉS, *Discretization of hyperelasticity on unstructured mesh with a cell-centered Lagrangian scheme.* J. Comp. Phys., 2010.

Outcome

- Satisfaction of the Piola compatibility condition **everywhere**
- **Consistency** and **continuity** of the Eulerian normal G***N***

Example of the fluid flow mapping in the fourth order case

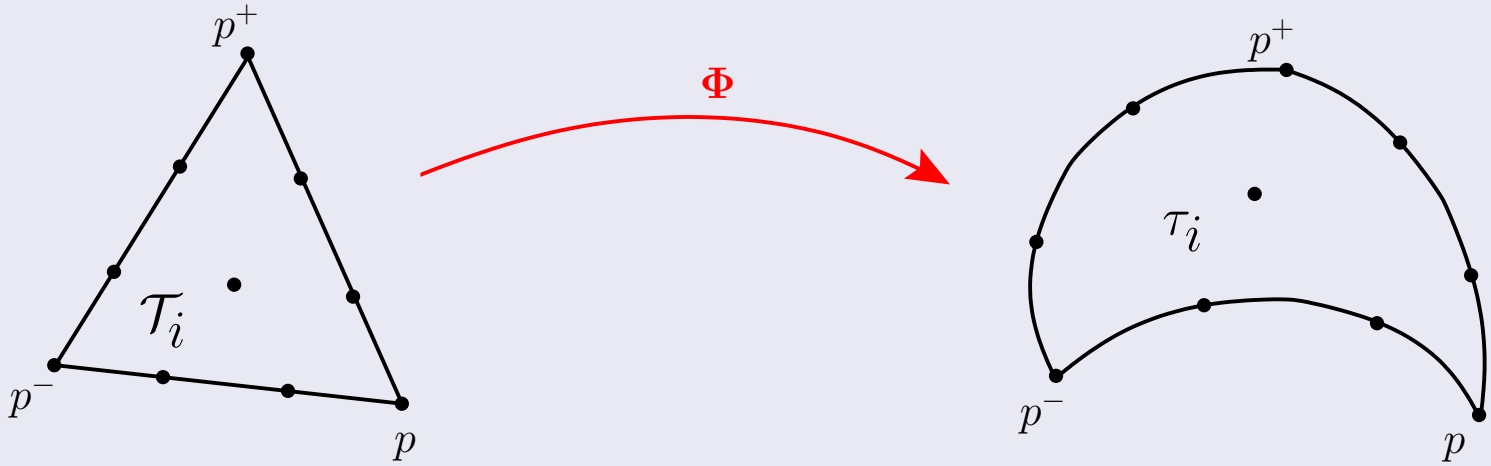

Figure: Nodes arrangement for a cubic Lagrange Finite Element mapping.

Curved edges definition using $s+1$ control points

- Projection of the continuous mapping function Φ on the face f_{pp^+}

$$\boldsymbol{x}_{|_{pp^+}}(\zeta) = \boldsymbol{x}_p \lambda_p(\zeta) + \sum_{q \in \mathcal{Q}(pp^+) \setminus \{p, p^+\}} \boldsymbol{x}_q \lambda_q(\zeta) \quad + \boldsymbol{x}_{p^+} \lambda_{p^+}(\zeta),$$

where $\mathcal{Q}(pp^+)$ is the face control points set, $\zeta \in [0,1]$ the curvilinear abscissa and λ_q the 1D Finite Element basis functions of degree s

Local variational formulations

- $$\int_{\Omega_c} \rho^0 \frac{\mathrm{d}\,\phi}{\mathrm{d}t} \sigma_j^c \,\mathrm{d}V = -\sum_{i=1}^{ntri} \int_{\mathcal{T}_i^c} \mathsf{G}\,\nabla_X \sigma_j^c \,.\, \boldsymbol{f}\,\mathrm{d}V + \sum_{p \in \mathcal{P}(c)} \int_p^{p^+} \bar{\boldsymbol{f}} \,.\, \sigma_j^c \,\mathsf{G}\boldsymbol{N}\mathrm{d}L$$

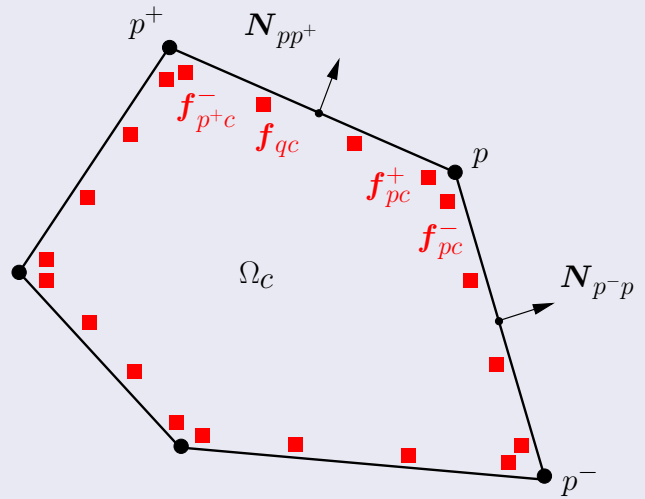

Polynomial assumptions on face f_{pp^+}

- $$\boldsymbol{f}_{|_{pp^+}}(\zeta) = \boldsymbol{f}^+_{pc}\lambda_p(\zeta) + \sum_{q\setminus\{p,p^+\}} \boldsymbol{f}_{qc}\lambda_q(\zeta) \quad + \boldsymbol{f}^-_{p^+c}\lambda_{p^+}(\zeta)$$

Polynomial properties on face f_{pp^+}

- $$\mathsf{G}\,\boldsymbol{N}\,\mathrm{d}L_{|_{pp^+}}(\zeta) = \boldsymbol{n}\,\mathrm{d}l_{|_{pp^+}} = \frac{\partial \boldsymbol{x}}{\partial \zeta}\mathrm{d}\zeta_{|_{pp^+}} \times \boldsymbol{e}_z = \sum_q \frac{\partial \lambda_q}{\partial \zeta}(\zeta)\,(\boldsymbol{x}_q \times \boldsymbol{e}_z)$$
- $$\sigma^c_{j|_{pp^+}}(\zeta) = \sigma_j^c(\boldsymbol{X}_p)\lambda_p(\zeta) + \sum_{q\setminus\{p,p^+\}} \sigma_j^c(\boldsymbol{X}_q)\lambda_q(\zeta) \quad + \sigma_j^c(\boldsymbol{X}_{p^+})\lambda_{p^+}(\zeta)$$

Fundamental assumptions

- $\boldsymbol{U}_{pc}^{\pm} = \boldsymbol{U}_p, \quad \forall c \in \mathcal{C}(p) \quad \text{and} \quad \boldsymbol{U}_{qL} = \boldsymbol{U}_{qR} = \boldsymbol{U}_q$
- $\overline{P\boldsymbol{U}} = \overline{P}\,\overline{\boldsymbol{U}} \quad \Longrightarrow \quad (P\boldsymbol{U})_{pc}^{\pm} = P_{pc}^{\pm}\,\boldsymbol{U}_p \quad \text{and} \quad (P\boldsymbol{U})_{qc} = P_{qc}\,\boldsymbol{U}_q$

Procedure

- Analytical integration + index permutation

Weighted control point normals

- $l_{pc}^{+,j}\,\boldsymbol{n}_{pc}^{+,j} = \left(\int_0^1 \lambda_{p|_{pp^+}}(\zeta)\sigma_{j|_{pp^+}}(\zeta)\,\frac{\partial \boldsymbol{x}}{\partial \zeta}\mathrm{d}\zeta_{|_{pp^+}}\right) \times \boldsymbol{e}_z$
- $l_{pc}^{-,j}\,\boldsymbol{n}_{pc}^{-,j} = \left(\int_0^1 \lambda_{p|_{p^-p}}(\zeta)\sigma_{j|_{p^-p}}(\zeta)\,\frac{\partial \boldsymbol{x}}{\partial \zeta}\mathrm{d}\zeta_{|_{p^-p}}\right) \times \boldsymbol{e}_z$
- $l_{pc}^{j}\boldsymbol{n}_{pc}^{j} = l_{pc}^{-,j}\,\boldsymbol{n}_{pc}^{-,j} + l_{pc}^{+,j}\,\boldsymbol{n}_{pc}^{+,j}$
- $l_{qc}^{j}\boldsymbol{n}_{qc}^{j} = \left(\int_0^1 \lambda_{q|_{pp^+}}(\zeta)\sigma_{j|_{pp^+}}(\zeta)\,\frac{\partial \boldsymbol{x}}{\partial \zeta}\mathrm{d}\zeta_{|_{pp^+}}\right) \times \boldsymbol{e}_z$

j^{th} moment of the subcell forces

- $\boldsymbol{F}_{pc}^{j} = P_{pc}^{-}\,l_{pc}^{-,j}\,\boldsymbol{n}_{pc}^{-,j} + P_{pc}^{+}\,l_{pc}^{+,j}\,\boldsymbol{n}_{pc}^{+,j} \quad \text{and} \quad \boldsymbol{F}_{qc}^{j} = P_{qc}\,l_{qc}^{j}\boldsymbol{n}_{qc}^{j}$

Semi-discrete equations GCL compatible

$$\int_{\Omega_c} \rho^0 \frac{\mathrm{d}}{\mathrm{d}t}\left(\frac{1}{\rho}\right)\sigma_j^c \,\mathrm{d}V = -\sum_{i=1}^{ntri} \int_{\mathcal{T}_i^c} \boldsymbol{U}\,.\,\mathrm{G}\nabla_X \sigma_j^c \mathrm{d}V + \sum_{p\in\mathcal{P}(c)} \left(\boldsymbol{U}_p\,.\,l_{pc}^j \boldsymbol{n}_{pc}^j + \sum_{q\setminus\{p,p^+\}} \boldsymbol{U}_q\,.\,l_{qc}^j \boldsymbol{n}_{qc}^j \right)$$

$$\int_{\Omega_c} \rho^0 \frac{\mathrm{d}\,\boldsymbol{U}}{\mathrm{d}t}\sigma_j^c \,\mathrm{d}V = \sum_{i=1}^{ntri} \int_{\mathcal{T}_i^c} P\mathrm{G}\nabla_X \sigma_j^c \mathrm{d}V - \sum_{p\in\mathcal{P}(c)} \left(\boldsymbol{F}_{pc}^j + \sum_{q\setminus\{p,p^+\}} \boldsymbol{F}_{qc}^j \right)$$

$$\int_{\Omega_c} \rho^0 \frac{\mathrm{d}\,E}{\mathrm{d}t}\sigma_j^c \,\mathrm{d}V = \sum_{i=1}^{ntri} \int_{\mathcal{T}_i^c} P\boldsymbol{U}\,.\,\mathrm{G}\nabla_X \sigma_j^c \mathrm{d}V - \sum_{p\in\mathcal{P}(c)} \left(\boldsymbol{U}_p\,.\,\boldsymbol{F}_{pc}^j + \sum_{q\setminus\{p,p^+\}} \boldsymbol{U}_q\,.\,\boldsymbol{F}_{qc}^j \right)$$

Equation on the first moment of the specific volume

- $$\frac{\mathrm{d}\,|\omega_c|}{\mathrm{d}t} = \int_{\partial\Omega_c} \overline{\boldsymbol{U}}\,.\,\mathrm{G}\boldsymbol{N}\mathrm{d}L = \sum_{p\in\mathcal{P}(c)} \left(\boldsymbol{U}_p\,.\,l_{pc}^0 \boldsymbol{n}_{pc}^0 + \sum_{q\in\mathcal{Q}(pp^+)\setminus\{p,p^+\}} \boldsymbol{U}_q\,.\,l_{qc}^0 \boldsymbol{n}_{qc}^0 \right)$$

Entropic semi-discrete equation

- Fundamental assumption $\overline{P\,\boldsymbol{U}} = \overline{P}\,\overline{\boldsymbol{U}}$
- The use of variational formulations and Piola condition leads to

$$\int_{\Omega_c} \rho^0\,\theta \frac{\mathrm{d}\,\eta}{\mathrm{d}t}\,\mathrm{d}V = \int_{\partial\Omega_c} (\overline{P} - P_h)(\boldsymbol{U}_h - \overline{\boldsymbol{U}})\,.\,\mathrm{G}\boldsymbol{N}\mathrm{d}S,$$

where η is the specific entropy and θ the absolute temperature defined by means of the Gibbs identity

Entropic semi-discrete equation

- A sufficient condition to satisfy $\int_{\Omega_c} \rho^0\,\theta \frac{\mathrm{d}\,\eta}{\mathrm{d}t}\,\mathrm{d}V \geq 0$ is

$$\overline{P} - P_h = -Z\,(\overline{\boldsymbol{U}} - \boldsymbol{U}_h)\,.\,\frac{\mathrm{G}\boldsymbol{N}}{\|\mathrm{G}\boldsymbol{N}\|} = -Z\,(\overline{\boldsymbol{U}} - \boldsymbol{U}_h)\,.\,\boldsymbol{n},$$

where $Z \geq 0$ has the physical dimension of a density times a velocity

Subcell forces definitions

- $\boldsymbol{F}_{pc}^{j} = P_{pc}^{-} \, l_{pc}^{-,j} \boldsymbol{n}_{pc}^{-,j} + P_{pc}^{+} \, l_{pc}^{+,j} \boldsymbol{n}_{pc}^{+,j}$ and $\boldsymbol{F}_{qc}^{j} = P_{qc} \, l_{qc}^{j} \boldsymbol{n}_{qc}^{j}$

j^{th} moment of the control point subcell forces

- The use of $\overline{P} = P_h^c - Z_c \, (\overline{\boldsymbol{U}} - \boldsymbol{U}_h^c) \cdot \boldsymbol{n}$ to calculate $\boldsymbol{F}_{pc}^{j}$ and $\boldsymbol{F}_{qc}^{j}$ leads to

$$\boldsymbol{F}_{pc}^{j} = P_h^c(\boldsymbol{X}_p, t) \, l_{pc}^{j} \boldsymbol{n}_{pc}^{j} - \mathrm{M}_{pc}^{j} \, (\boldsymbol{U}_p - \boldsymbol{U}_h^c(\boldsymbol{X}_p, t)),$$

$$\boldsymbol{F}_{qc}^{j} = P_h^c(\boldsymbol{X}_q, t) \, l_{qc}^{j} \boldsymbol{n}_{qc}^{j} - \mathrm{M}_{qc}^{j} \, (\boldsymbol{U}_q - \boldsymbol{U}_h^c(\boldsymbol{X}_q, t)),$$

$\mathrm{M}_{pc}^{j} = Z_c \left(l_{pc}^{-,j} \boldsymbol{n}_{pc}^{-,j} \otimes \boldsymbol{n}_{pc}^{-,0} + l_{pc}^{+,j} \boldsymbol{n}_{pc}^{+,j} \otimes \boldsymbol{n}_{pc}^{+,0} \right)$ and $\mathrm{M}_{qc}^{j} = Z_c \, l_{qc}^{j} \boldsymbol{n}_{qc}^{j} \otimes \boldsymbol{n}_{qc}^{0}$

Momentum and total energy conservation

- $\sum_{c \in \mathcal{C}(p)} \boldsymbol{F}_{pc}^{0} = \boldsymbol{0}$ and $\boldsymbol{F}_{qL}^{0} + \boldsymbol{F}_{qR}^{0} = \boldsymbol{0}$

Nodal velocity

- $M_p \, \boldsymbol{U}_p = \sum_{c \in \mathcal{C}(p)} \left[P_h^c(\boldsymbol{X}_p, t) \, l_{pc}^0 \boldsymbol{n}_{pc}^0 + \mathrm{M}_{pc}^0 \, \boldsymbol{U}_h^c(\boldsymbol{X}_p, t) \right],$

  where $\mathrm{M_p} = \sum_{c \in \mathcal{C}(p)} \mathrm{M}_{pc}^0$ is a **positive definite** matrix

Face control point velocity

- $\mathrm{M}_q \, \boldsymbol{U}_q = \mathrm{M}_q \left(\dfrac{Z_L \, \boldsymbol{U}_h^L(\boldsymbol{X}_q) + Z_R \, \boldsymbol{U}_h^R(\boldsymbol{X}_q)}{Z_L + Z_R} \right) - \dfrac{P_h^R(\boldsymbol{X}_q) - P_h^L(\boldsymbol{X}_q)}{Z_L + Z_R} \, l_{qL}^0 \boldsymbol{n}_{qL}^0,$

  where $\mathrm{M}_q = \frac{1}{Z_R} \mathrm{M}_{qR}^0 = \frac{1}{Z_L} \mathrm{M}_{qL}^0 = l_{qL}^0 \boldsymbol{n}_{qL}^0 \otimes \boldsymbol{n}_{qL}^0$ is **positive semi-definite**

1D approximate Riemann problem solution

- $(\boldsymbol{U}_q \cdot \boldsymbol{n}_{qL}^0) = \left(\dfrac{Z_L \, \boldsymbol{U}_h^L(\boldsymbol{X}_q) + Z_R \, \boldsymbol{U}_h^R(\boldsymbol{X}_q)}{Z_L + Z_R} \right) \cdot \boldsymbol{n}_{qL}^0 - \dfrac{P_h^R(\boldsymbol{X}_q) - P_h^L(\boldsymbol{X}_q)}{Z_L + Z_R}$

Tangential component of the face control point velocity

- $(\boldsymbol{U}_q \cdot \boldsymbol{t}^0_{qL}) = \left(\dfrac{Z_L \boldsymbol{U}^L_h(\boldsymbol{X}_q) + Z_R \boldsymbol{U}^R_h(\boldsymbol{X}_q)}{Z_L + Z_R} \right) \cdot \boldsymbol{t}^0_{qL}$

Face control point velocity

- $\boldsymbol{U}_q = \dfrac{Z_L \boldsymbol{U}^L_h(\boldsymbol{X}_q) + Z_R \boldsymbol{U}^R_h(\boldsymbol{X}_q)}{Z_L + Z_R} - \dfrac{P^R_h(\boldsymbol{X}_q) - P^L_h(\boldsymbol{X}_q)}{Z_L + Z_R} \boldsymbol{n}^0_{qL}$

Deformation tensor

- $\dfrac{\mathrm{d}}{\mathrm{d}t}\mathsf{F}_i = \sum_{Q \in \mathcal{Q}(i)} \boldsymbol{U}_Q \otimes \boldsymbol{\nabla}_X \Lambda^i_Q$

Interior points velocity

- $\boldsymbol{U}_Q = \boldsymbol{U}^c_h(\boldsymbol{X}_Q, t)$

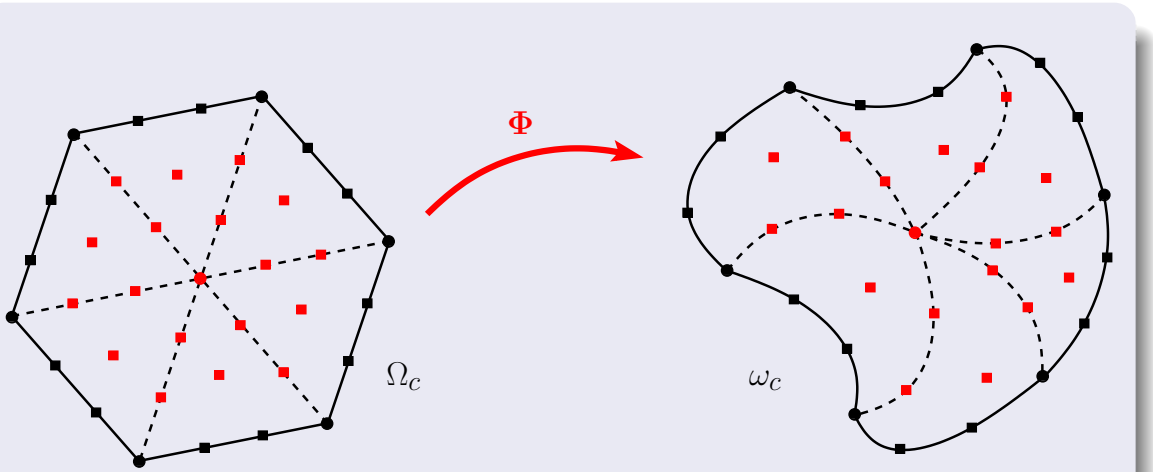

Riemann invariants differentials

- $\mathrm{d}\alpha_t = \mathrm{d}\boldsymbol{U} \cdot \boldsymbol{t}$
- $\mathrm{d}\alpha_- = \mathrm{d}(\frac{1}{\rho}) - \frac{1}{\rho a}\,\mathrm{d}\boldsymbol{U} \cdot \boldsymbol{n}$
- $\mathrm{d}\alpha_+ = \mathrm{d}(\frac{1}{\rho}) + \frac{1}{\rho a}\,\mathrm{d}\boldsymbol{U} \cdot \boldsymbol{n}$
- $\mathrm{d}\alpha_E = \mathrm{d}E - \boldsymbol{U} \cdot \mathrm{d}\boldsymbol{U} + P\,\mathrm{d}(\frac{1}{\rho})$

a denotes the sound speed

Mean value linearization

- $\alpha^c_{t,h} = \boldsymbol{U}^c_h \cdot \boldsymbol{t}$
- $\alpha^c_{-,h} = (\frac{1}{\rho})^c_h - \frac{1}{Z_c}\,\boldsymbol{U}^c_h \cdot \boldsymbol{n}$
- $\alpha^c_{+,h} = (\frac{1}{\rho})^c_h + \frac{1}{Z_c}\,\boldsymbol{U}^c_h \cdot \boldsymbol{n}$
- $\alpha^c_{E,h} = E^c_h - \boldsymbol{U}^c_0 \cdot \boldsymbol{U}^c_h + P^c_0\,(\frac{1}{\rho})^c_h$

where $Z_c = a^c_0 \rho^c_0$

System variables polynomial approximation components

- $(\frac{1}{\rho})^c_k = \frac{1}{2}(\alpha^c_{+,k} + \alpha^c_{-,k})$
- $\boldsymbol{U}^c_k = \frac{1}{2} Z_c (\alpha^c_{+,k} - \alpha^c_{-,k})\boldsymbol{n} + \alpha^c_{t,k}\boldsymbol{t}$
- $E^c_k = \alpha^c_{E,k} + \frac{1}{2} Z_c (\alpha^c_{+,k} - \alpha^c_{-,k})\boldsymbol{U}^c_0 \cdot \boldsymbol{n} + \alpha^c_{t,k}\boldsymbol{U}^c_0 \cdot \boldsymbol{t} - \frac{1}{2} P^c_0 (\alpha^c_{+,k} + \alpha^c_{-,k})$

Unit direction ensuring symmetry preservation

- $\boldsymbol{n} = \dfrac{\boldsymbol{U}^c_0}{\|\boldsymbol{U}^c_0\|}$ and $\boldsymbol{t} = \boldsymbol{e}_z \times \dfrac{\boldsymbol{U}^c_0}{\|\boldsymbol{U}^c_0\|}$

Composed derivatives

- $\mathsf{F}_T = \nabla_{X_r} \Phi_T(\boldsymbol{X}_r, t)$
  $= \nabla_X \Phi_H(\boldsymbol{X}, t) \circ \nabla_{X_r} \Phi_0(\boldsymbol{X}_r)$
  $= \mathsf{F}_H \mathsf{F}_0$
- $J_T(\boldsymbol{X}_r, t) = J_H(\boldsymbol{X}, t)\, J_0(\boldsymbol{X}_r)$

Mass conservation

- $\rho^0\, J_0 = \rho\, J_T$

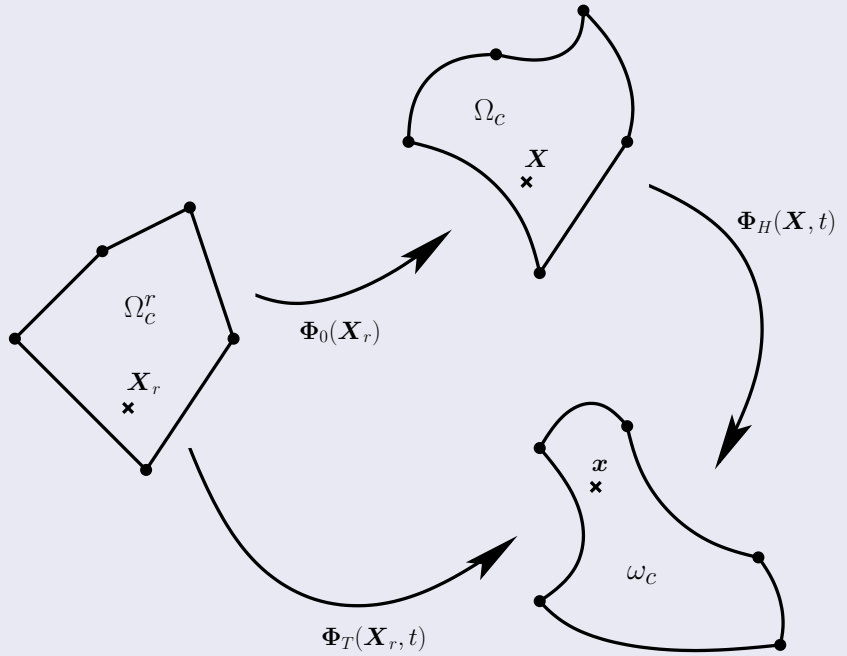

Modification of the mass matrix

- $\displaystyle\int_{\omega_c} \rho\, \frac{\mathrm{d}\,\psi_h^c}{\mathrm{d}t}\, \sigma_j\, \mathrm{d}\omega = \sum_{k=0}^{K} \frac{\mathrm{d}\,\psi_k}{\mathrm{d}t} \int_{\Omega_c^r} \rho^0\, J_0\, \sigma_j\, \sigma_k\, \mathrm{d}\Omega^r$ time rate of change of successive moments of function ψ
- New definitions of mass matrix, of mass averaged value and of the associated scalar product

Sedov point blast problem on a Cartesian grid

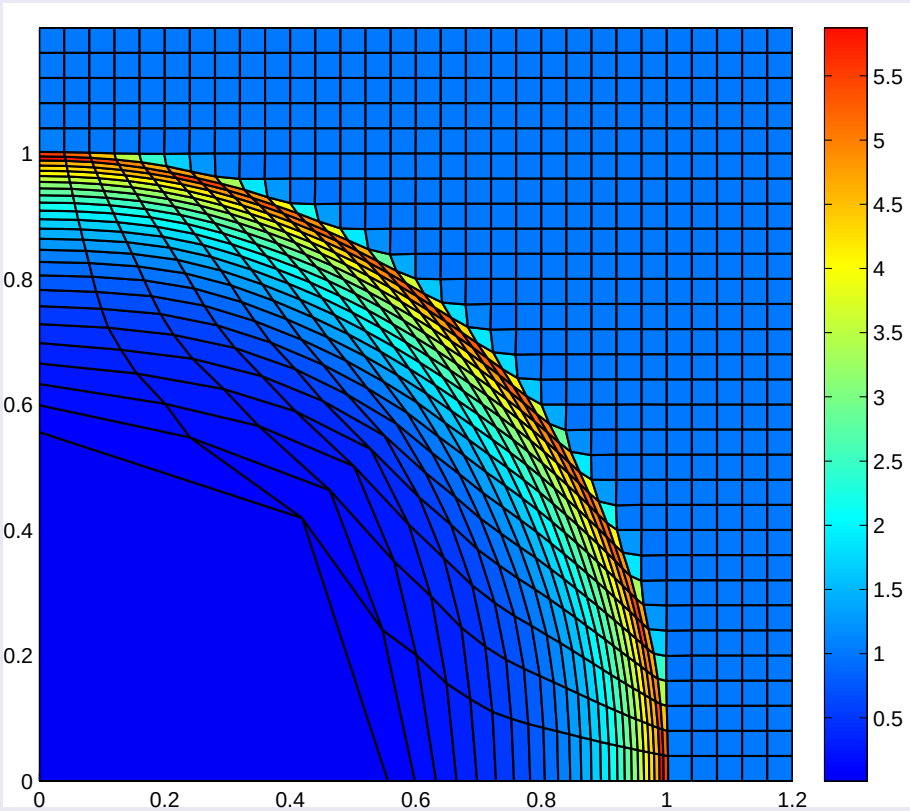

(a) Second-order scheme.

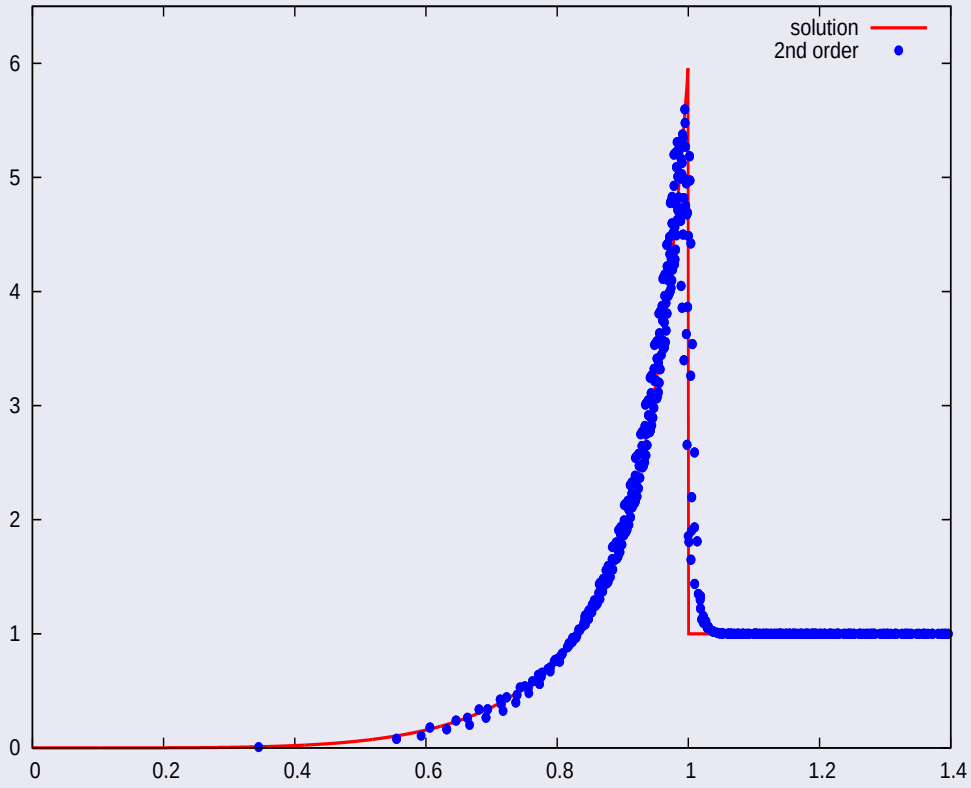

(b) Density profile.

Figure: Point blast Sedov problem on a Cartesian grid made of 30 $\times$ 30 cells: density.

Sedov point blast problem on unstructured grids

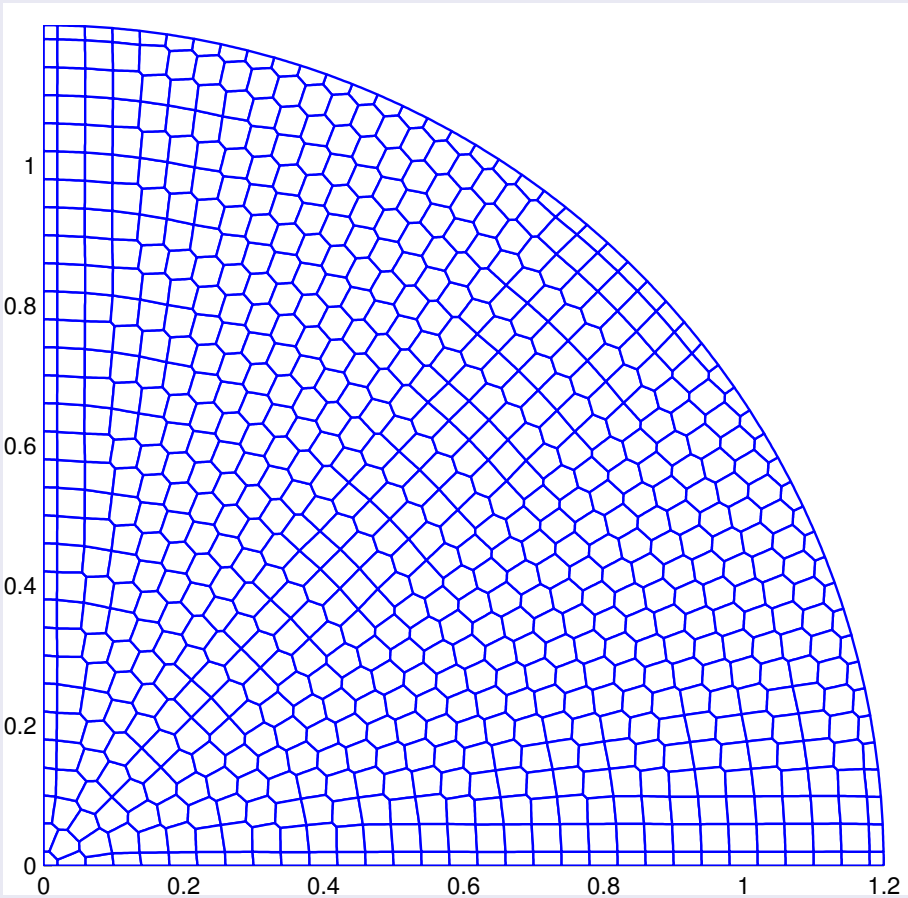

(a) Polygonal grid.

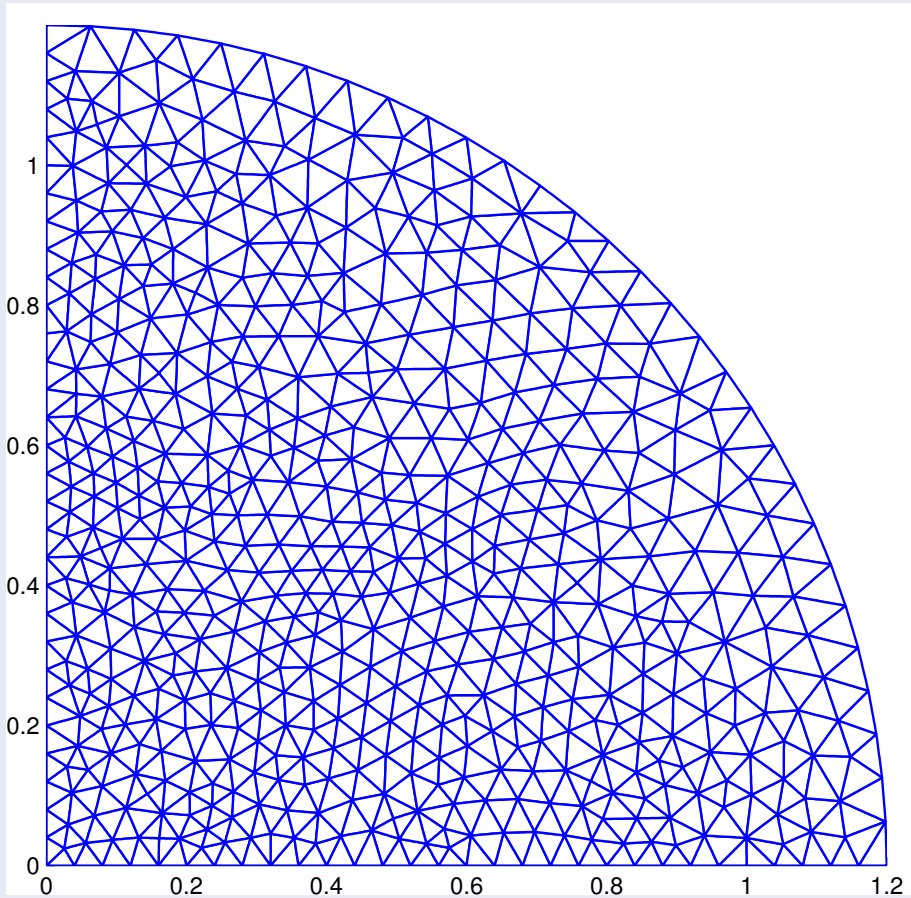

(b) Triangular grid.

Figure: Unstructured initial grids for the point blast Sedov problem.

Sedov point blast problem a polygonal grid

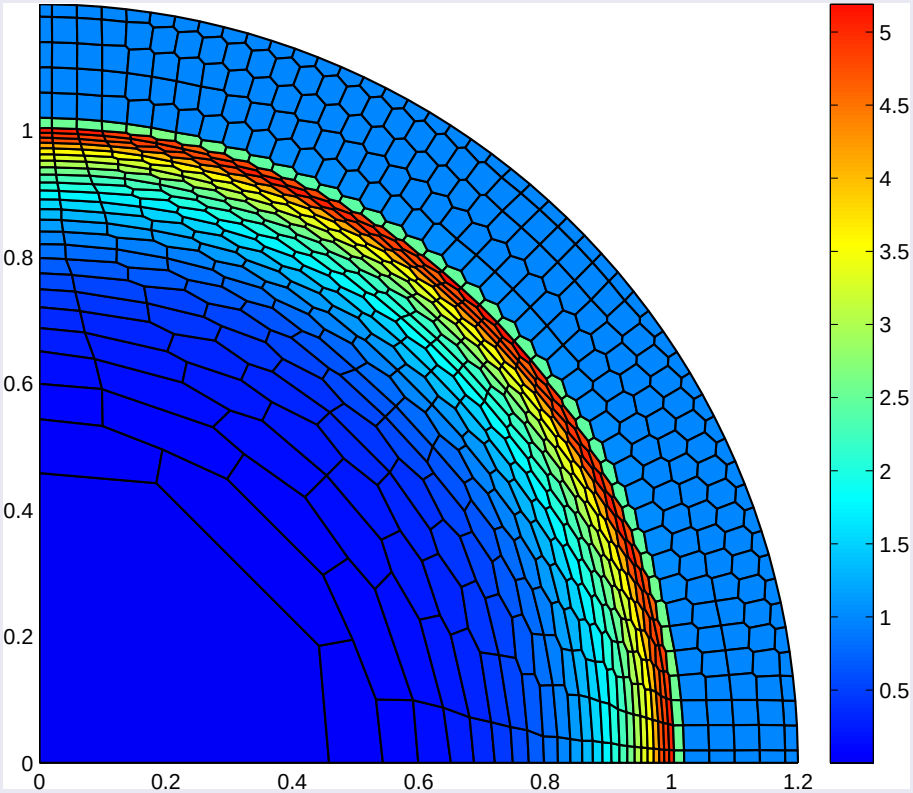

(a) Second-order scheme.

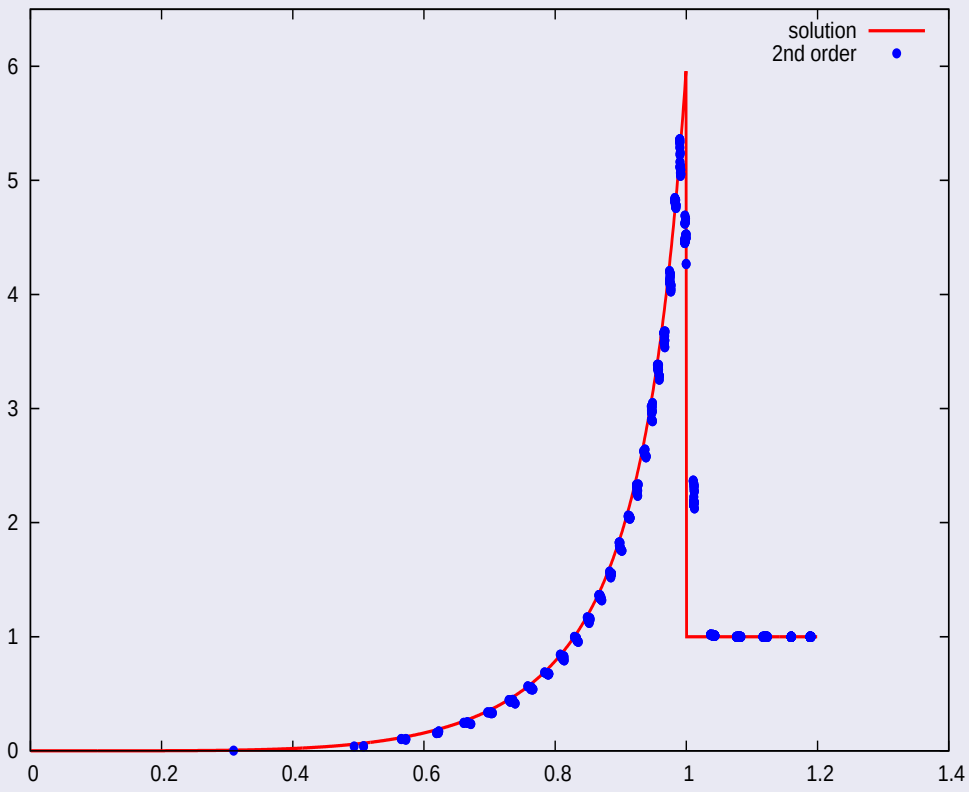

(b) Density profile.

Figure: Point blast Sedov problem on an unstructured grid made of 775 polygonal cells: density map.

Sedov point blast problem on a triangular grid

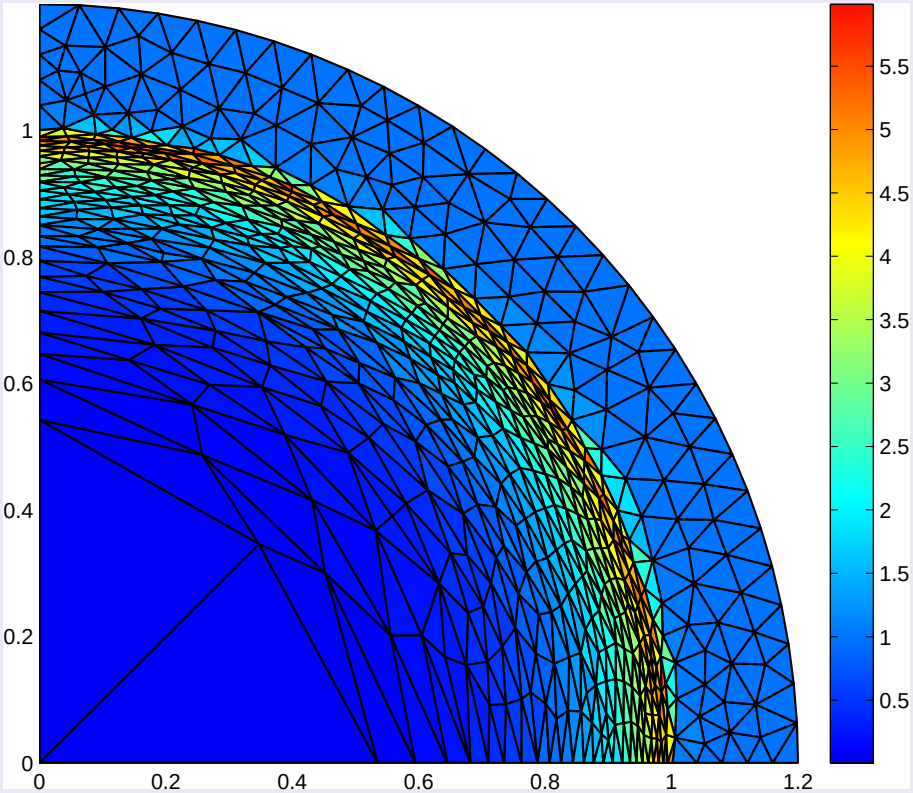

(a) Second-order scheme.

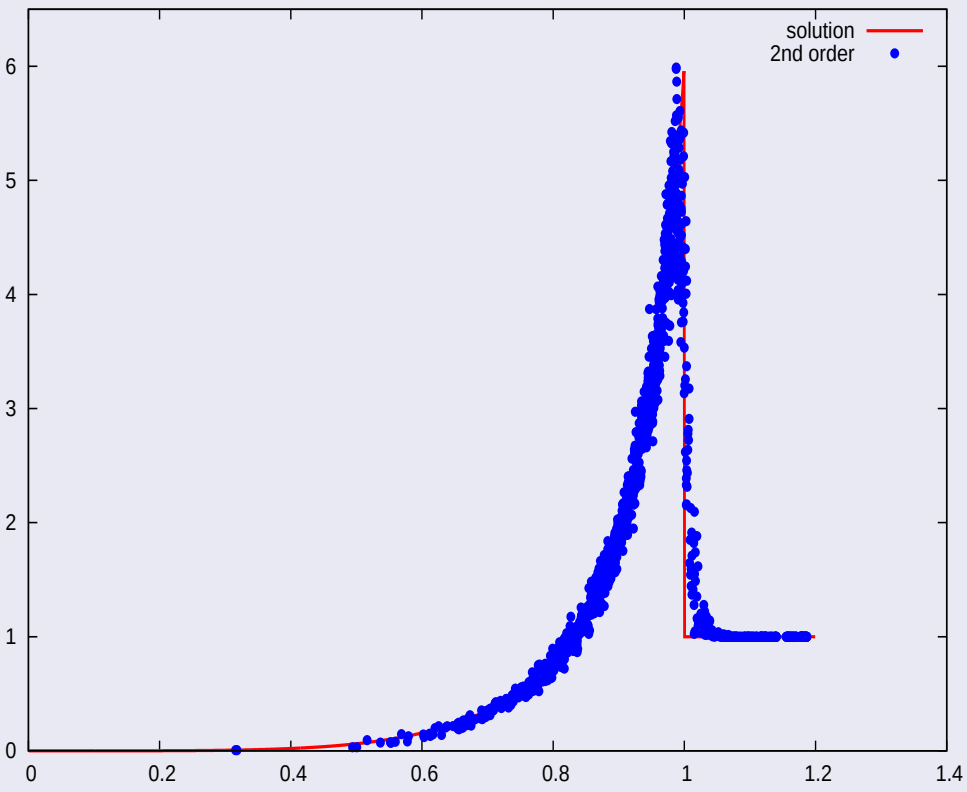

(b) Density profile.

Figure: Point blast Sedov problem on an unstructured grid made of 1100 triangular cells: density map.

Noh problem

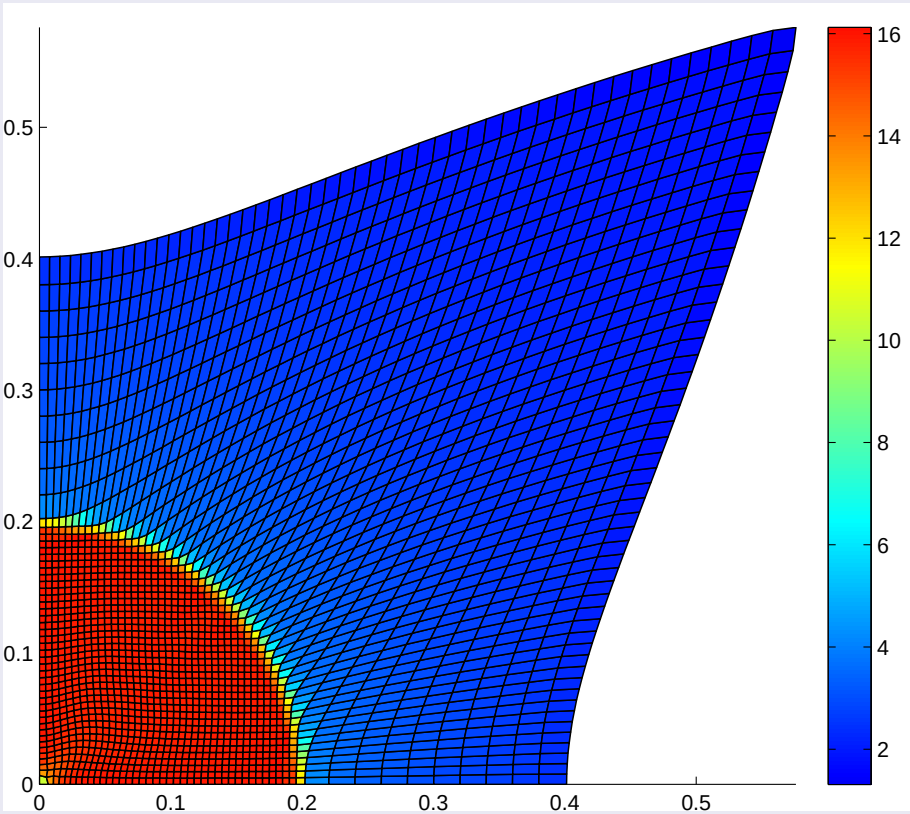

(a) Second-order scheme.

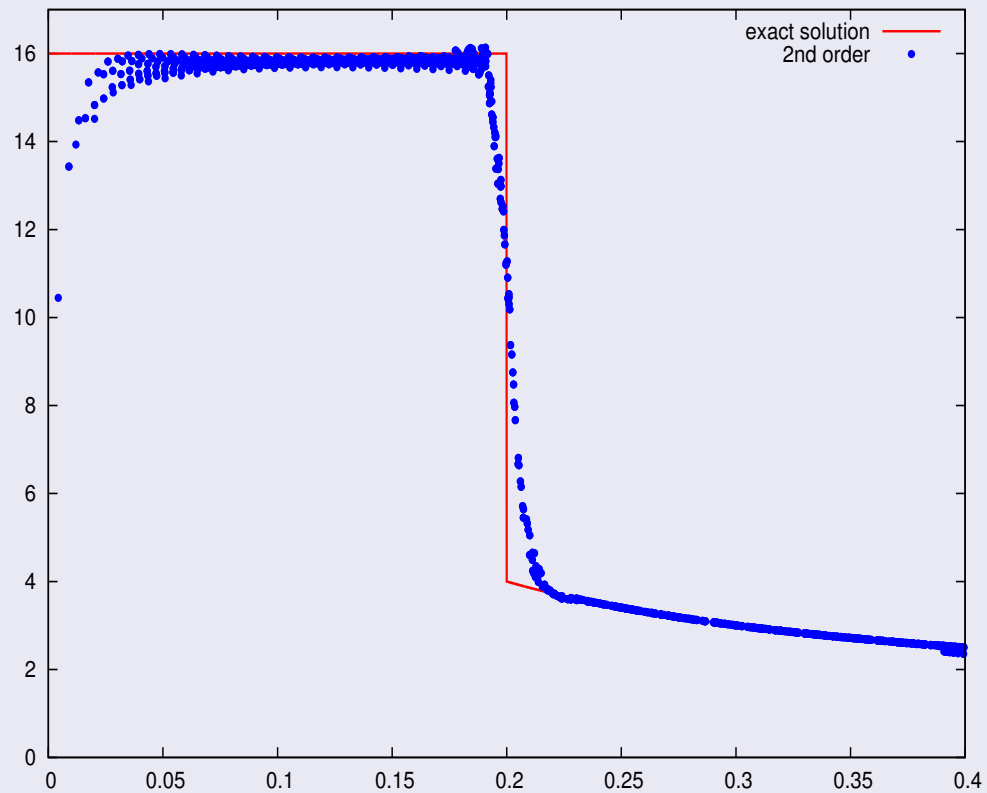

(b) Density profile.

Figure: Noh problem on a Cartesian grid made of 50×50 cells: density.

Taylor-Green vortex problem, introduced by R. Rieben (LLNL)

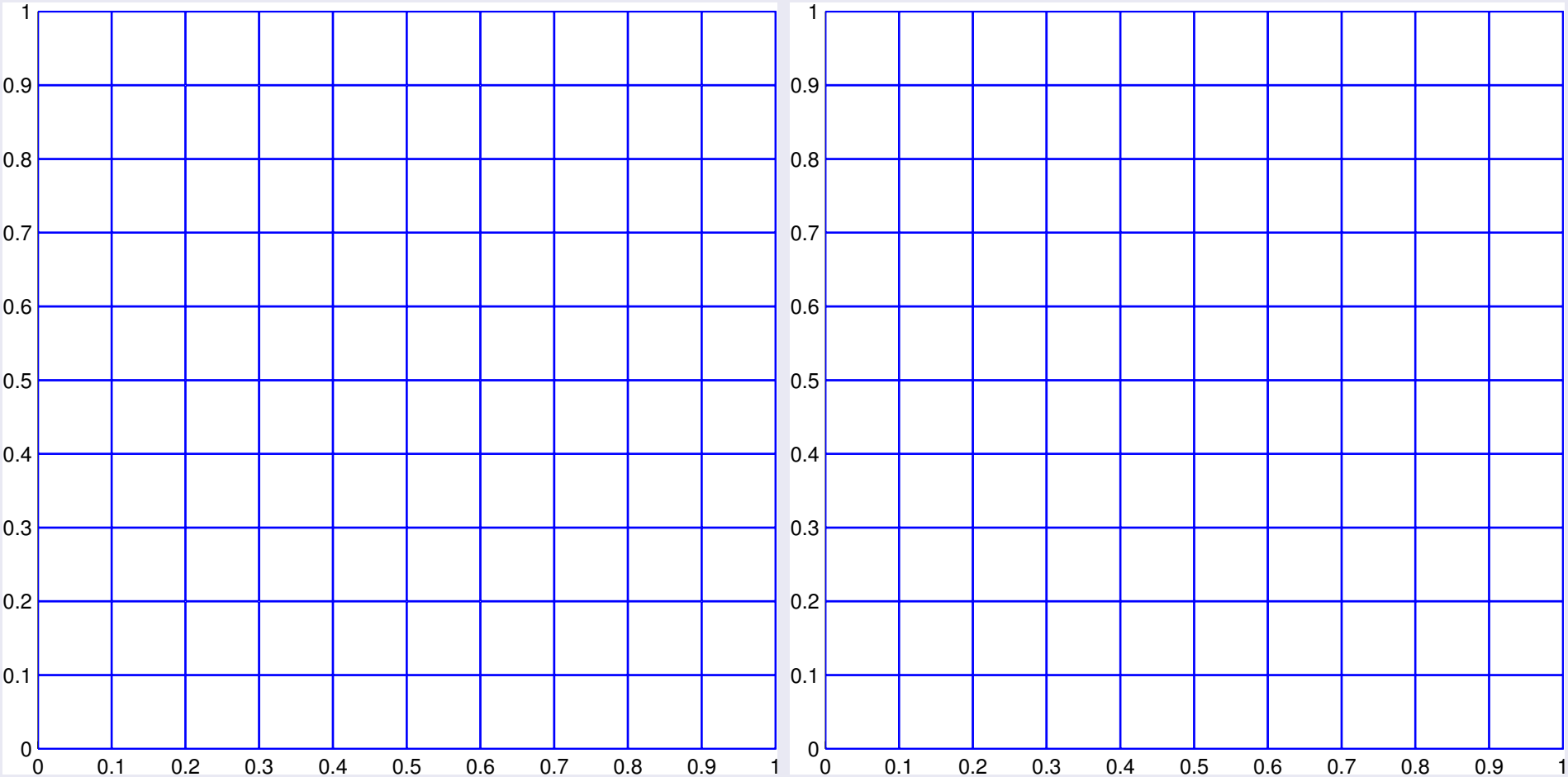

(a) Second-order scheme. (b) Exact solution.

Figure: Motion of a 10×10 Cartesian mesh through a T.-G. vortex, at $t = 0.75$.

Taylor-Green vortex problem

	L_1		L_2		L_∞	
h	$E^h_{L_1}$	$q^h_{L_1}$	$E^h_{L_2}$	$q^h_{L_2}$	$E^h_{L_\infty}$	$q^h_{L_\infty}$
$\frac{1}{10}$	5.06E-3	1.94	6.16E-3	1.93	2.20E-2	1.84
$\frac{1}{20}$	1.32E-3	1.98	1.62E-3	1.97	5.91E-3	1.95
$\frac{1}{40}$	3.33E-4	1.99	4.12E-4	1.99	1.53E-3	1.98
$\frac{1}{80}$	8.35E-5	2.00	1.04E-4	2.00	3.86E-4	1.99
$\frac{1}{160}$	2.09E-5	-	2.60E-5	-	9.69E-5	-

Table: Rate of convergence computed on the pressure at time $t = 0.1$.

Polar grids

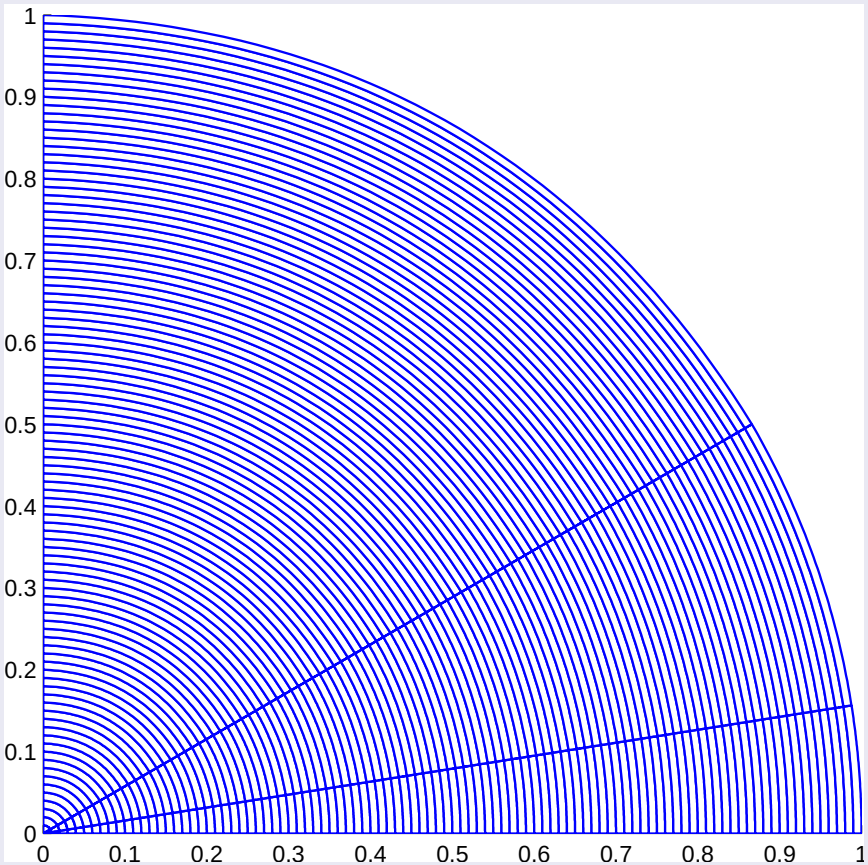

(a) Non-uniform grid.

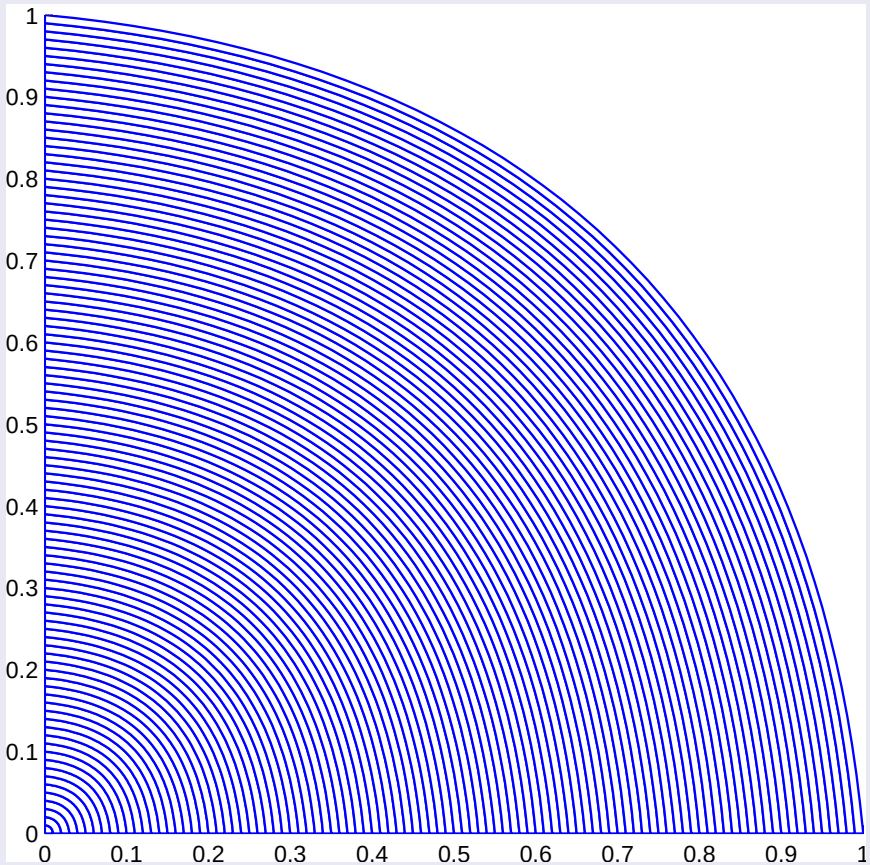

(b) One angular cell grid.

Figure: Polar initial grids for the Sod shock tube problem.

Symmetry preservation

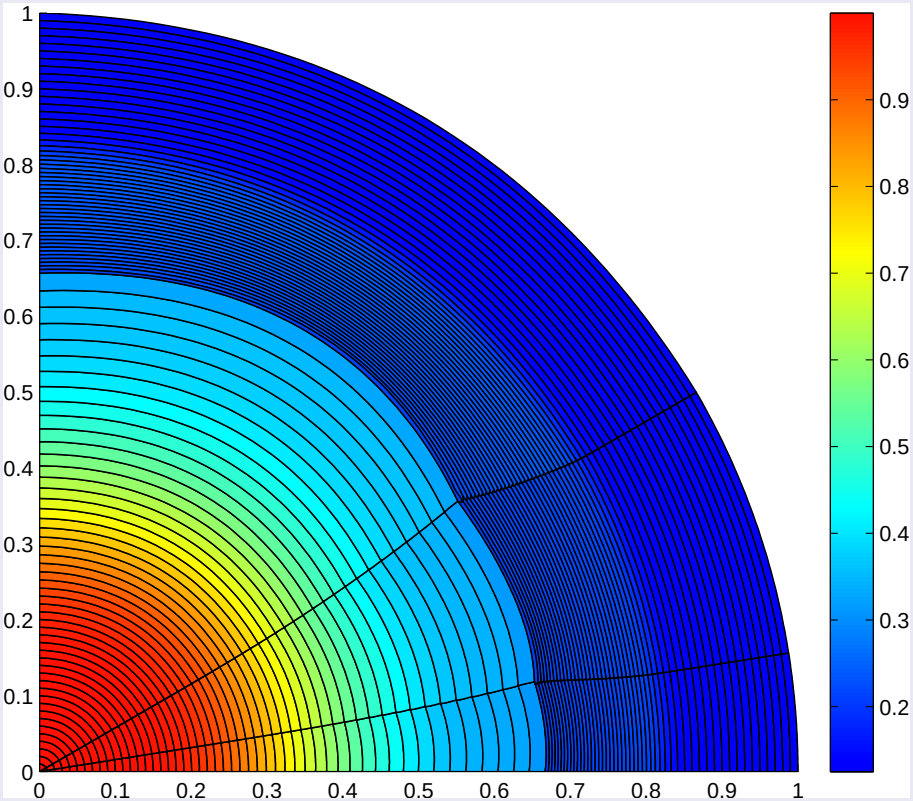

(a) First-order scheme.

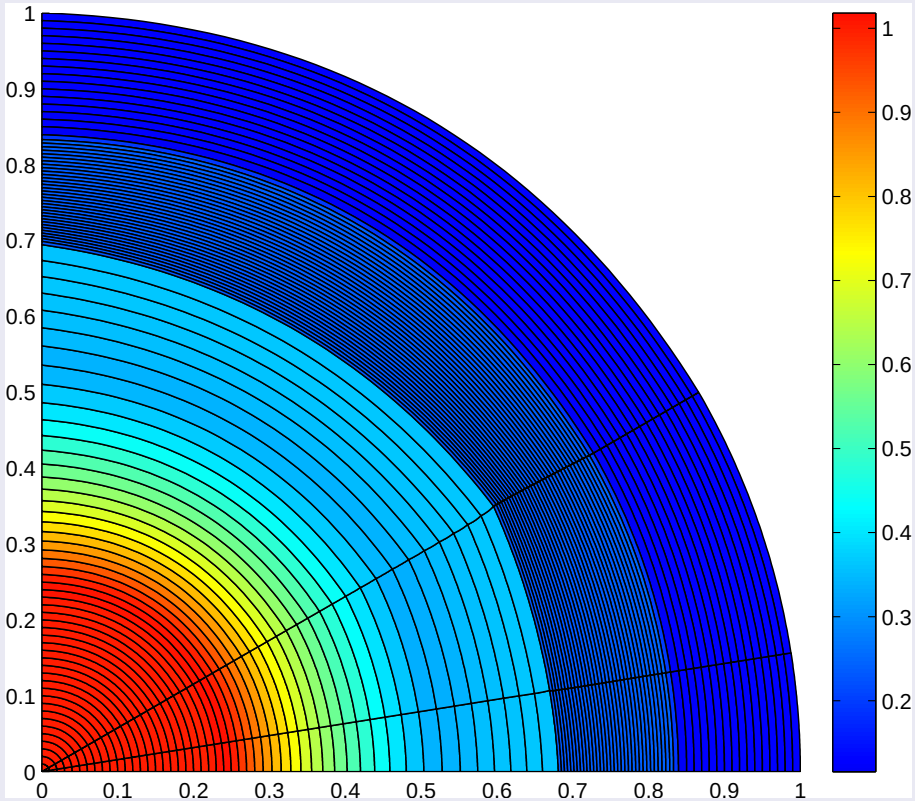

(b) Second-order scheme.

Figure: Sod shock tube problem on a polar grid made of 100 $\times$ 3 non-uniform cells.

Symmetry preservation

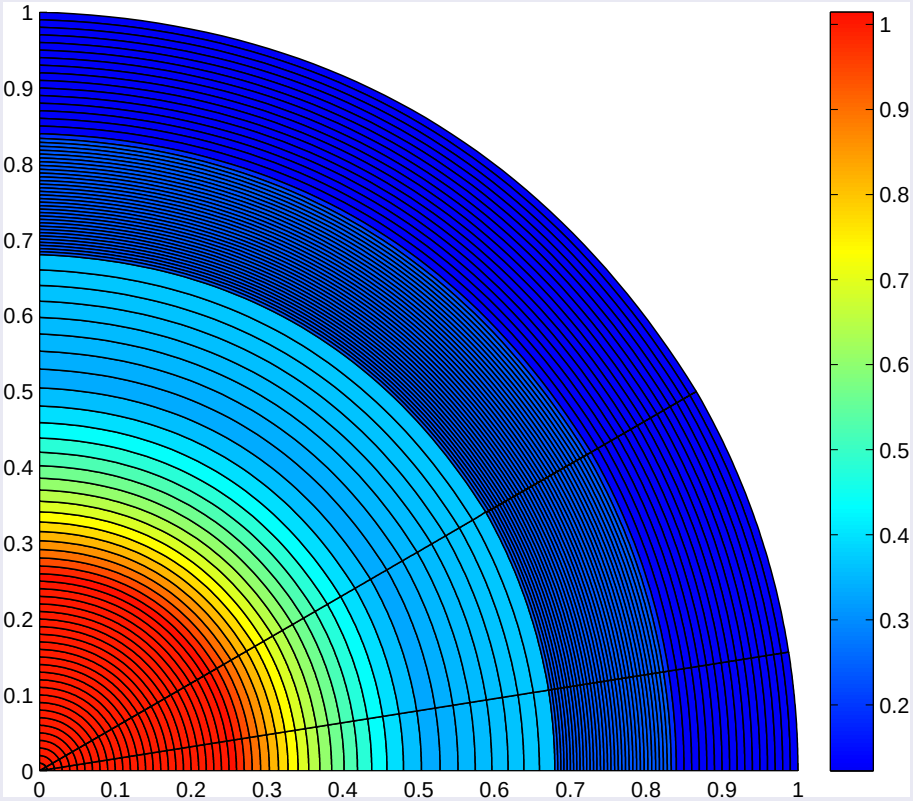

(a) Density map.

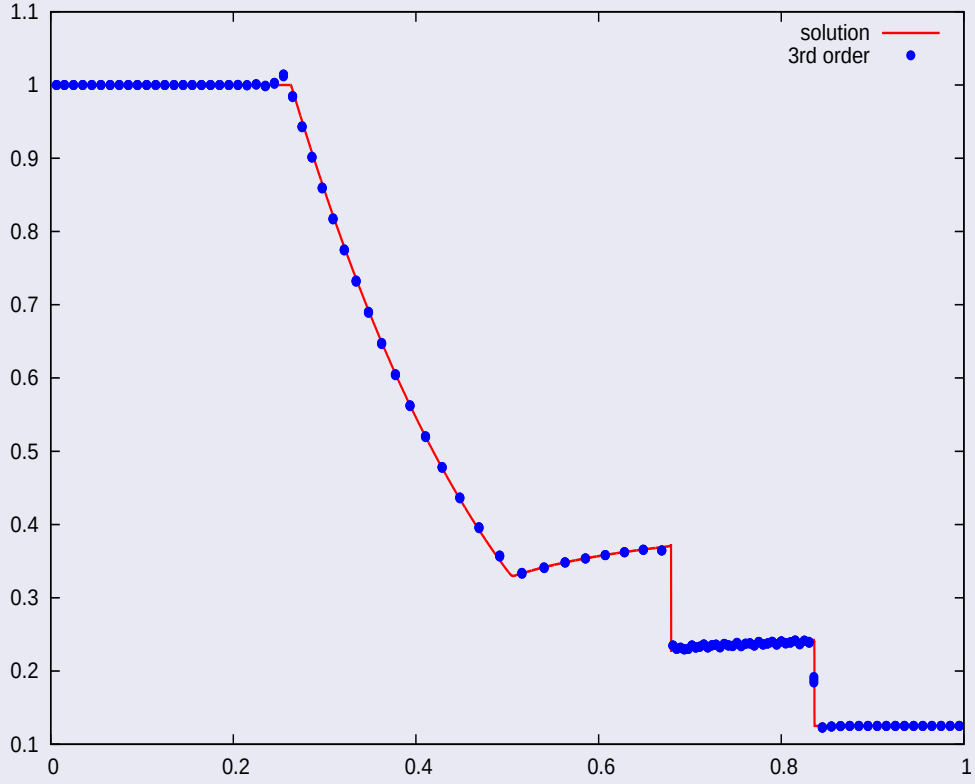

(b) Density profile.

Figure: Third-order DG solution for a Sod shock tube problem on a polar grid made of 100×3 non-uniform cells.

One angular cell polar Sod shock tube problem

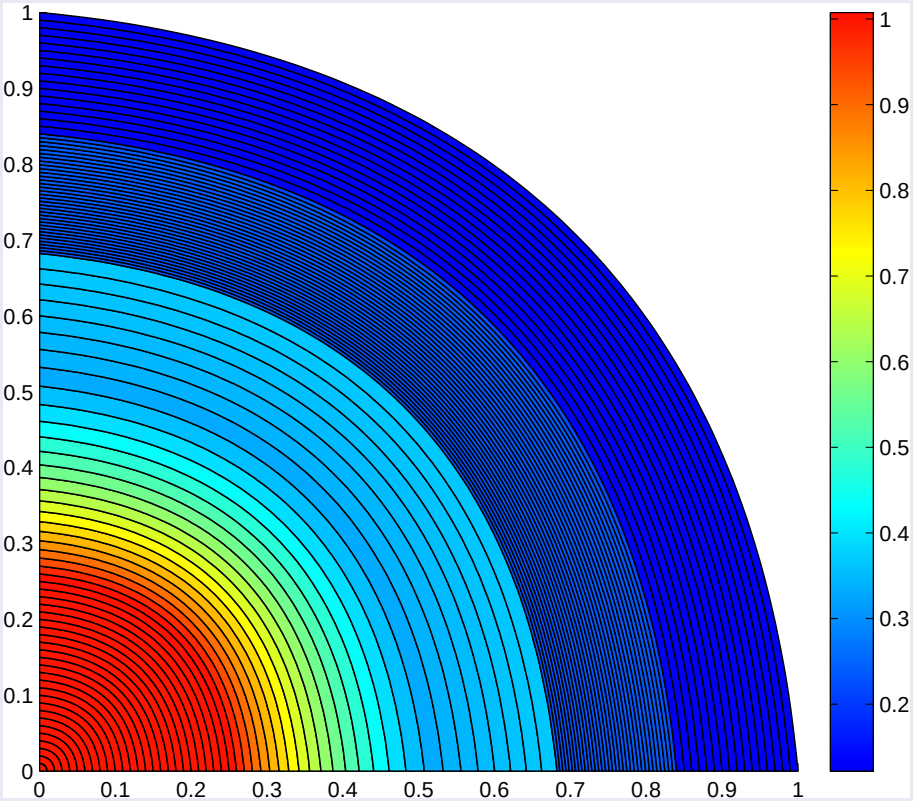

(a) Density map.

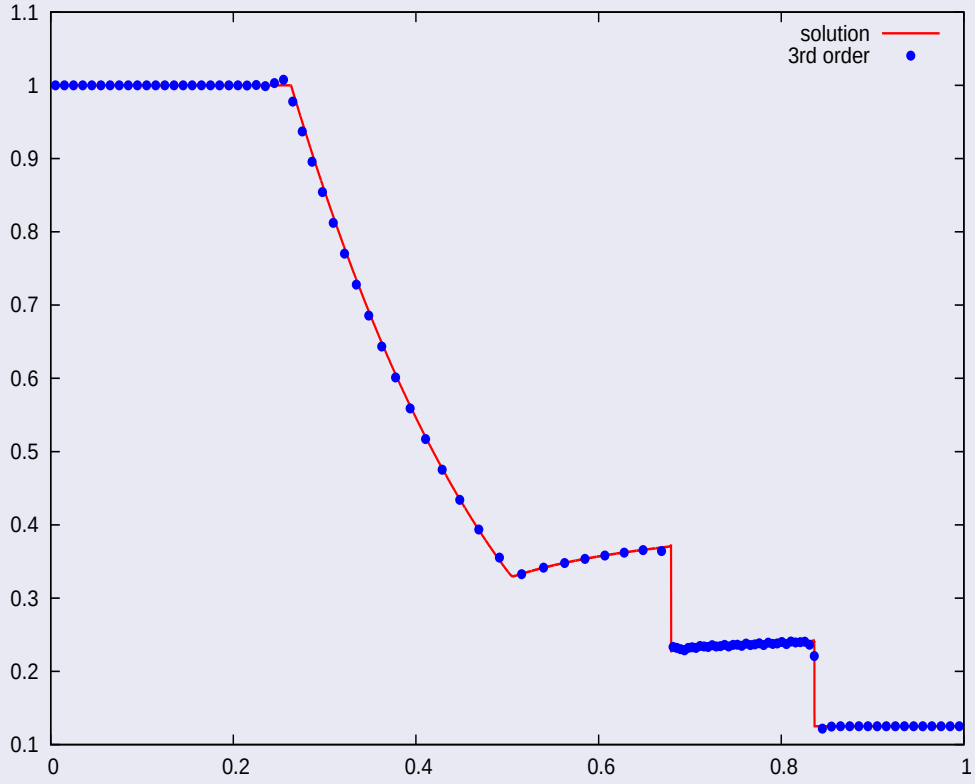

(b) Density profile.

Figure: Third-order DG solution for a Sod shock tube problem on a polar grid made of 100×1 cells.

Variant of the incompressible Gresho vortex problem

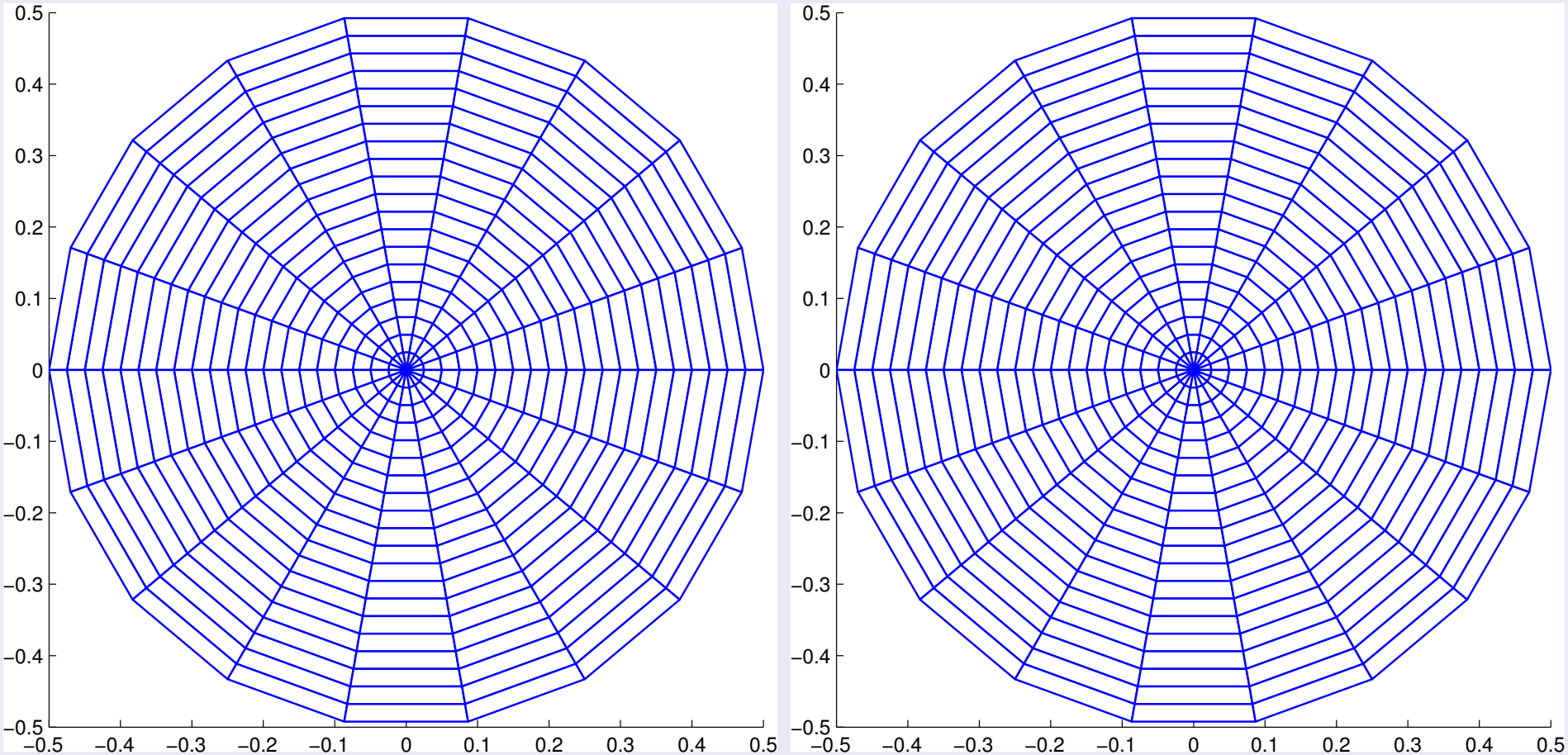

(a) First-order scheme. (b) Second-order scheme.

Figure: Motion of a polar grid defined in polar coordinates by $(r, \theta) \in [0, 1] \times [0, 2\pi]$, with 40×18 cells at $t = 1$: zoom on the zone $(r, \theta) \in [0, 0.5] \times [0, 2\pi]$.

Variant of the incompressible Gresho vortex problem

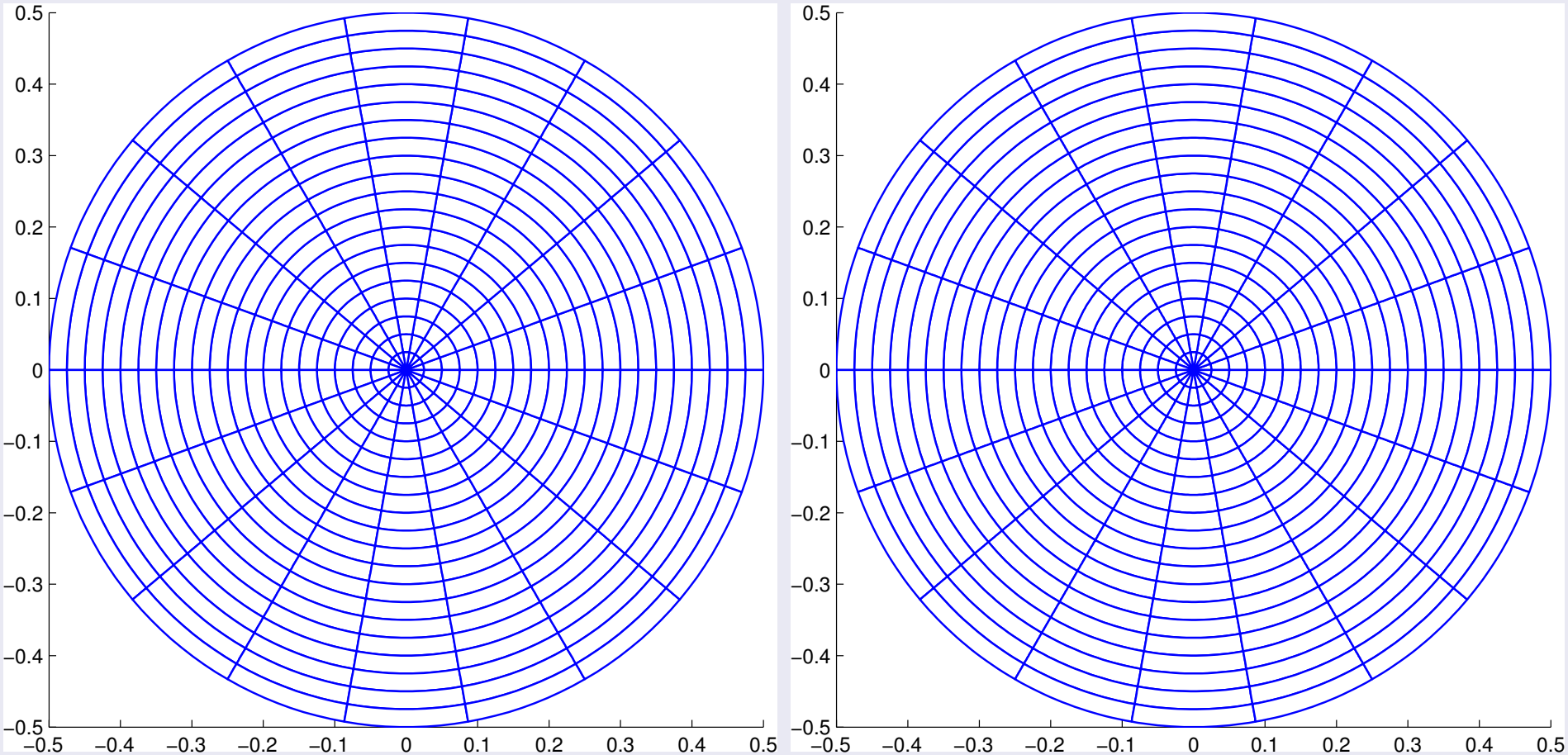

(a) Third-order scheme. (b) Exact solution.

Figure: Motion of a polar grid defined in polar coordinates by $(r, \theta) \in [0, 1] \times [0, 2\pi]$, with 40×18 cells at $t = 1$: zoom on the zone $(r, \theta) \in [0, 0.5] \times [0, 2\pi]$.

Variant of the Gresho vortex problem

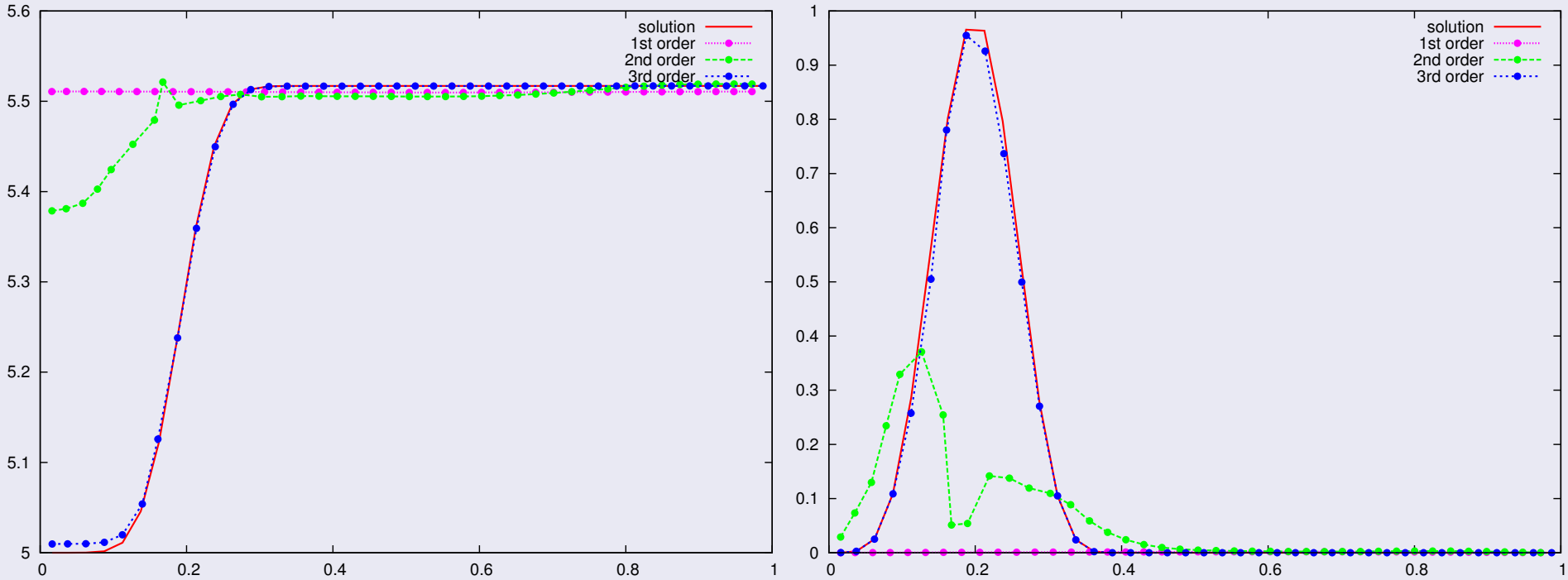

(a) Pressure profile.

(b) Velocity profile.

Figure: Gresho variant problem on a polar grid defined in polar coordinates by $(r, \theta) \in [0, 1] \times [0, 2\pi]$, with 40×18 cells at $t = 1$.

Variant of the Gresho vortex problem

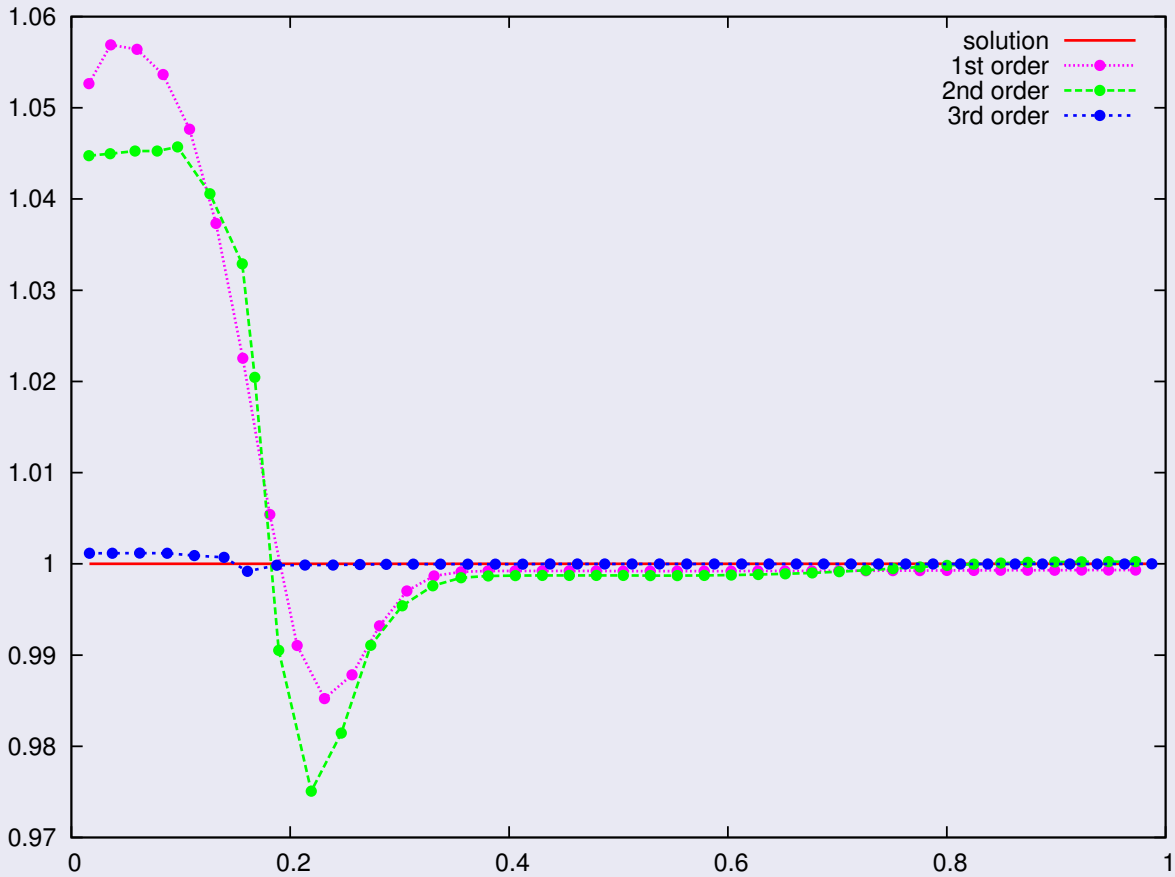

Figure: Gresho variant problem on a polar grid defined in polar coordinates by $(r, \theta) \in [0, 1] \times [0, 2\pi]$, with 40×18 cells at $t = 1$: density profile.

Kidder isentropic compression

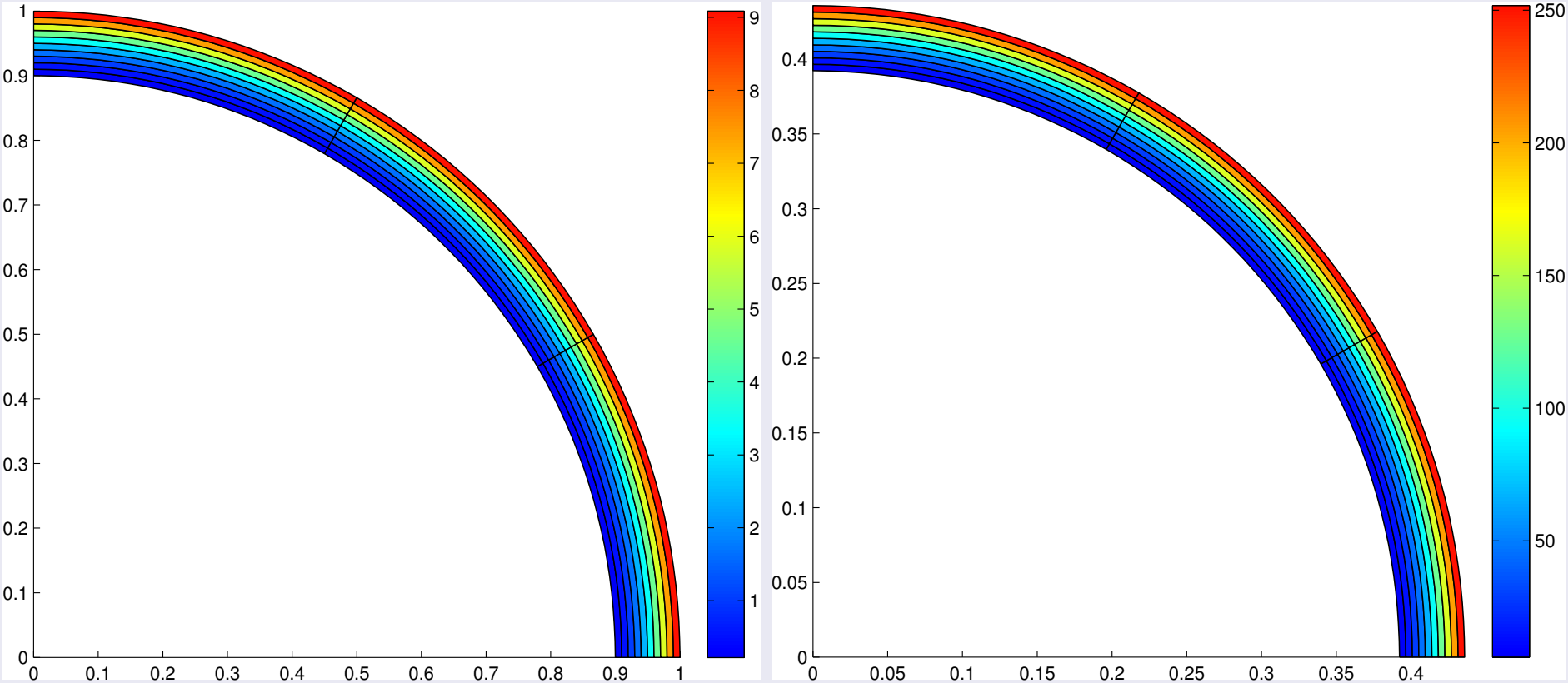

(a) At time $t = 0$.

(b) At time $t = 0.9\tau$.

Figure: Third-order DG solution for a Kidder isentropic compression problem on a polar grid made of 10×3 cells: pressure map.

Kidder isentropic compression

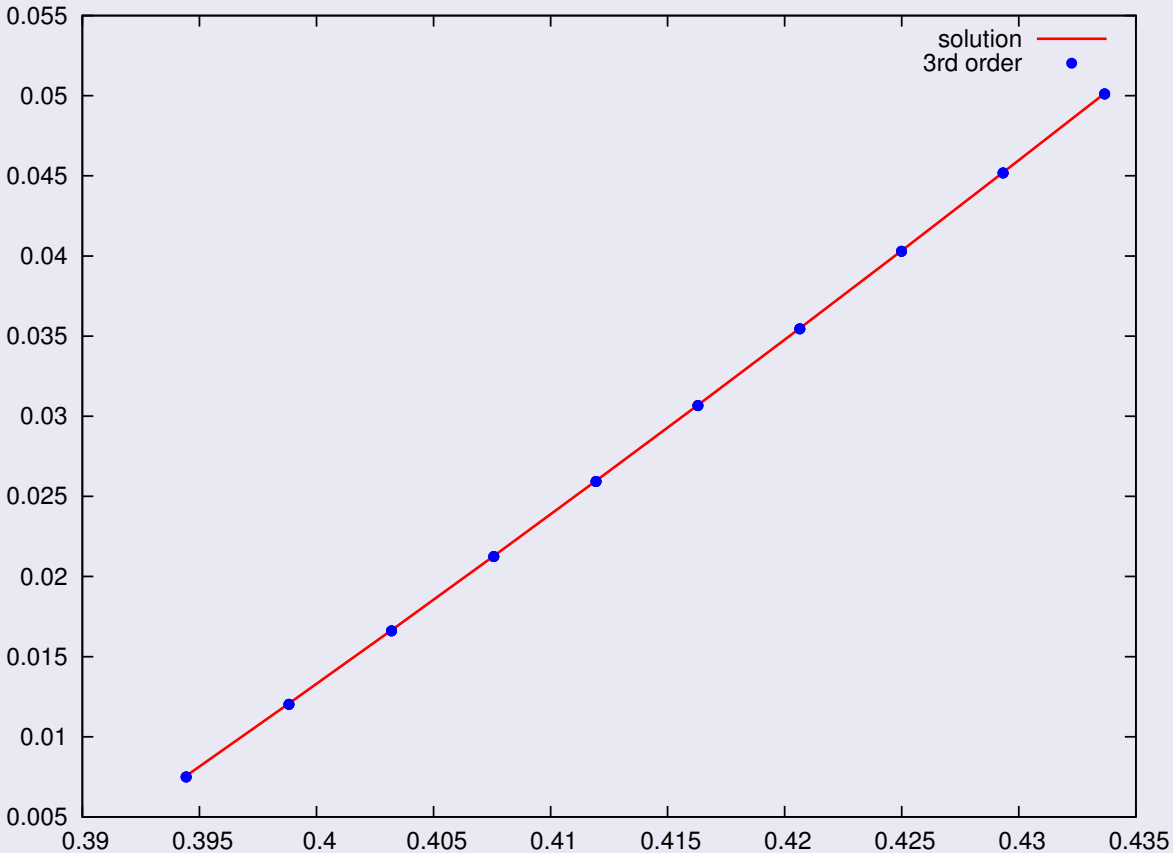

Figure: Third-order DG solution for a Kidder isentropic compression problem on a polar grid made of 10×3 cells: density profile.

Taylor-Green vortex problem

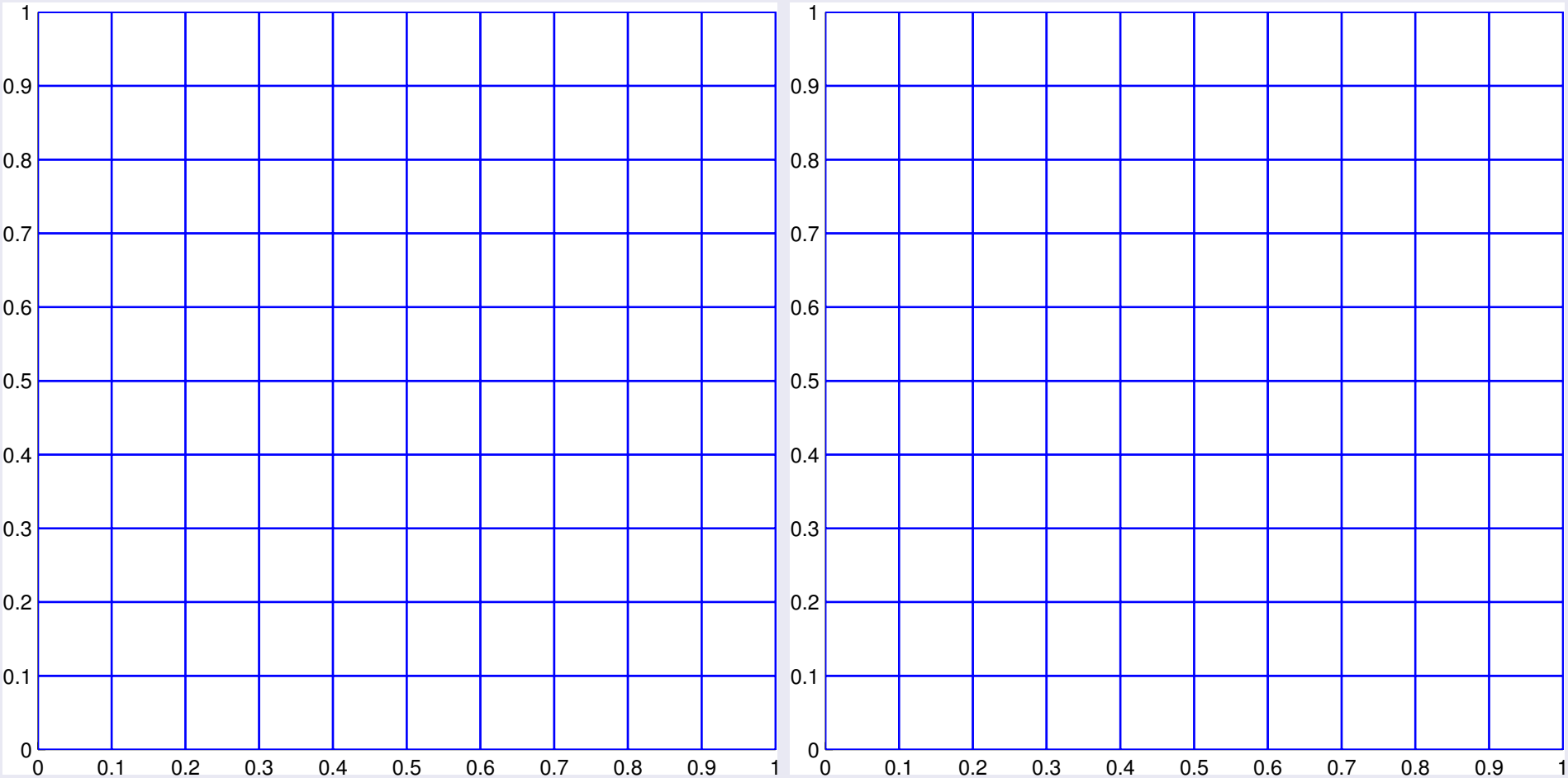

(a) Third-order scheme. (b) Exact solution.

Figure: Motion of a 10×10 Cartesian mesh through a T.-G. vortex, at $t = 0.75$.

Taylor-Green vortex problem

	L_1		L_2		L_∞	
h	$E^h_{L_1}$	$q^h_{L_1}$	$E^h_{L_2}$	$q^h_{L_2}$	$E^h_{L_\infty}$	$q^h_{L_\infty}$
$\frac{1}{10}$	2.67E-4	2.96	3.36E-4	2.94	1.21E-3	2.86
$\frac{1}{20}$	3.43E-5	2.97	4.36E-5	2.96	1.66E-4	2.93
$\frac{1}{40}$	4.37E-6	2.99	5.59E-6	2.98	2.18E-5	2.96
$\frac{1}{80}$	5.50E-7	2.99	7.06E-7	2.99	2.80E-6	2.99
$\frac{1}{160}$	6.91E-8	-	8.87E-8	-	3.53E-7	-

Table: Rate of convergence computed on the pressure at time $t = 0.1$.

Taylor-Green vortex problem

D.O.F	N	$E^h_{L_1}$	$E^h_{L_2}$	$E^h_{L_\infty}$	time (sec)
600	24×25	2.67E-2	3.31E-2	8.55E-2	2.01
2400	48×50	1.36E-2	1.69E-2	4.37E-2	11.0

Table: First-order DG scheme at time $t = 0.1$.

D.O.F	N	$E^h_{L_1}$	$E^h_{L_2}$	$E^h_{L_\infty}$	time (sec)
630	14×15	2.76E-3	3.33E-3	1.07E-2	2.77
2436	28×29	7.52E-4	9.02E-4	2.73E-3	11.3

Table: Second-order DG scheme without limitation at time $t = 0.1$.

D.O.F	N	$E^h_{L_1}$	$E^h_{L_2}$	$E^h_{L_\infty}$	time (sec)
600	10×10	2.67E-4	3.36E-4	1.21E-3	4.00
2400	20×20	3.43E-5	4.36E-5	1.66E-4	30.6

Table: Third-order DG scheme without limitation at time $t = 0.1$.

Sedov point blast problem on a Cartesian grid

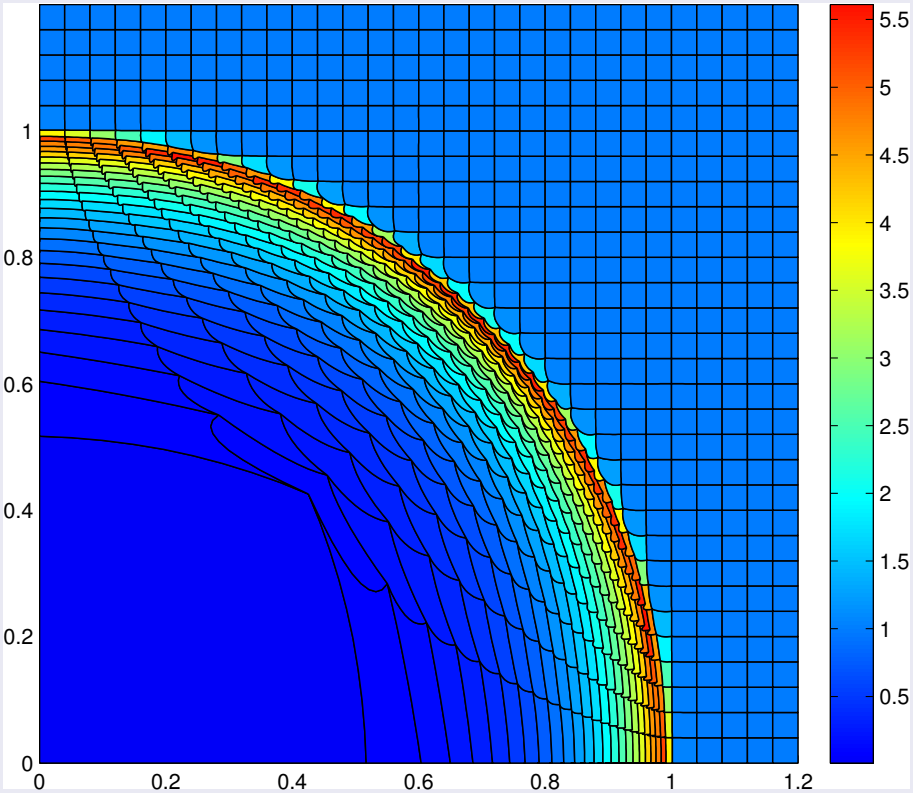

(a) Third-order scheme.

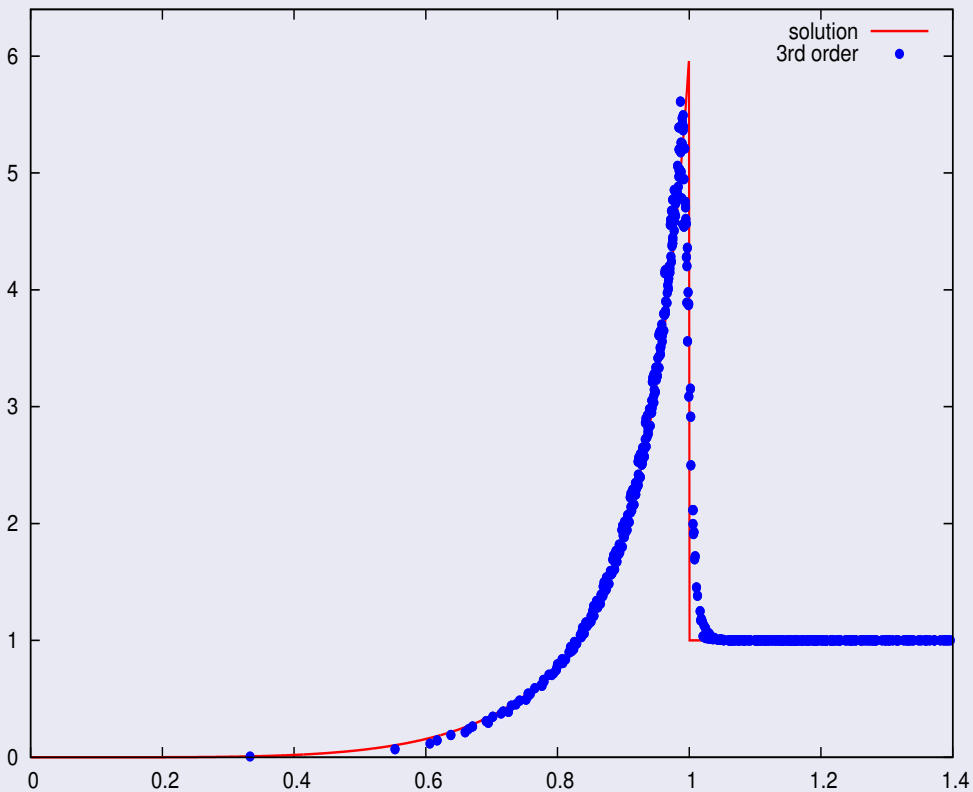

(b) Density profile.

Figure: Point blast Sedov problem on a Cartesian grid made of 30 $\times$ 30 cells: density.

Conclusions

- Development of 2nd and 3rd order DG schemes for the 2D gas dynamics system in a total Lagrangian formalism
- **GCL and Piola compatibility condition ensured by construction**
- **Dramatic improvement of symmetry preservation by means of third-order DG scheme**
- Riemann invariants limitation

Perspectives

- **High-order limitation**
  - Positivity preserving limitation
  - WENO limiter
- Code parallelization
- Development of a 3rd order DG scheme on moving mesh
- Extension to 3D
- Extension to ALE and solid dynamics


F. VILAR, P.-H. MAIRE AND R. ABGRALL, *Cell-centered discontinuous Galerkin discretizations for two-dimensional scalar conservation laws on unstructured grids and for one-dimensional Lagrangian hydrodynamics.* Computers and Fluids, 2010.


F. VILAR, *Cell-centered discontinuous Galerkin discretization for two-dimensional Lagrangian hydrodynamics.* Computers and Fluids, 2012.


F. VILAR, P.-H. MAIRE AND R. ABGRALL, *Third order Cell-Centered DG scheme for Lagrangian hydrodynamics on general unstructured Bezier grids.* Article in preparation.